

Energy levels, radiative rates and electron impact excitation rates for transitions in He-like Ga XXX, Ge XXXI, As XXXII, Se XXXIII and Br XXXIV

Kanti M Aggarwal and Francis P Keenan

Astrophysics Research Centre, School of Mathematics and Physics, Queen's University Belfast, Belfast BT7 1NN, Northern Ireland, UK

e-mail: K.Aggarwal@qub.ac.uk

Received 10 September 2012

Accepted for publication 06 March 2013

Published xx Month 2013

Online at stacks.iop.org/PhysScr/vol/number

PACS Ref: 32.70 Cs, 34.80 Dp, 95.30 Ky

S This article has associated online supplementary data files

Tables 2 and 4 are available only in the electronic version at stacks.iop.org/PhysScr/vol/number

Abstract

We report calculations of energy levels, radiative rates and electron impact excitation cross sections and rates for transitions in He-like Ga XXX, Ge XXXI, As XXXII, Se XXXIII and Br XXXIV. The GRASP (general-purpose relativistic atomic structure package) is adopted for calculating energy levels and radiative rates. For determining the collision strengths, and subsequently the excitation rates, the Dirac Atomic R-matrix Code (DARC) is used. Oscillator strengths, radiative rates and line strengths are reported for all E1, E2, M1 and M2 transitions among the lowest 49 levels of each ion. Additionally, theoretical lifetimes are provided for all 49 levels of the above five ions. Collision strengths are averaged over a Maxwellian velocity distribution and the effective collision strengths obtained listed over a wide temperature range up to 10^8 K. Comparisons are made with similar data obtained using the Flexible Atomic Code (FAC) to highlight the importance of resonances, included in calculations with DARC, in the determination of effective collision strengths. Discrepancies between the collision strengths from DARC and FAC, particularly for some forbidden transitions, are also discussed. Finally, discrepancies between the present results for effective collision strengths with the DARC code and earlier semi-relativistic R -matrix data are noted over a wide range of electron temperatures for many transitions in all ions.

1 Introduction

Emission lines of He-like ions have been widely observed from a variety of astrophysical and laboratory plasmas. For example, lines of many He-like ions detected in solar plasmas at x-ray wavelengths (1–50 Å) have been listed by Dere *et al* [1], and in the regions 170–211 Å and 245–291 Å by Feldman *et al* [2]. Similarly, transitions from these ions have been observed in laboratory plasmas [3] – [5]. Of particular interest are the resonance (w : $1s^2\ ^1S_0 - 1s2p\ ^1P_1^o$), intercombination (x and y : $1s^2\ ^1S_0 - 1s2p\ ^3P_{2,1}^o$), and forbidden (z : $1s^2\ ^1S_0 - 1s2s\ ^3S_1$) lines, which are highly useful for plasma diagnostics – see, for example, [6] – [9] and references therein. However, to analyse observations, atomic data are required for a variety of parameters, such as energy levels, radiative rates (A - values), and excitation rates or equivalently the effective collision strengths (Υ), which are obtained from the electron impact collision strengths (Ω). These data are also required for the modelling of fusion plasmas [10]. Therefore, in a series of papers we have already reported atomic data for He-like ions up to $Z=30$ [11] – [19] and for $Z=36$, i.e. Kr XXXV [20]. In this work we report similar data for the remaining five ions with $31 \leq Z \leq 35$, i.e. Ga XXX, Ge XXXI, As XXXII, Se XXXIII and Br XXXIV.

The National Institute of Standards and Technology (NIST) have compiled and critically evaluated energy levels for many He-like ions, and have posted data on their website <http://www.nist.gov/pml/data/asd.cfm>. Additionally, the A - value for the $1s^2\ ^1S_0 - 1s2s\ ^3S_1$ (1–2) magnetic dipole transition of Ga XXX is available on the NIST website. However, no collisional data are available in the literature for the ions under consideration. Therefore, in this paper we report a complete set of results (namely energy levels, radiative rates, lifetimes, and effective collision strengths) for all transitions among the lowest 49 fine-structure levels of these He-like ions, which belong to the $1s^2$, $1s2\ell$, $1s3\ell$, $1s4\ell$ and $1s5\ell$ configurations. Finally, we also provide the A - values for four types of transitions, namely electric dipole (E1), electric quadrupole (E2), magnetic dipole (M1) and magnetic quadrupole (M2), as these are required in a complete plasma model.

For our calculations we employ the fully relativistic GRASP (general-purpose relativistic atomic structure package) code for the determination of wavefunctions, originally developed by Grant *et al* [21] and subsequently revised by several workers, under the names GRASP [22], GRASP92 [23], and GRASP2K [24]. However, the version adopted here is GRASP0, which is based on [21] and is revised by Dr P H Norrington. This version contains most of the modifications undertaken in the other revised codes and is available on the website <http://web.am.qub.ac.uk/DARC/>. GRASP is a fully relativistic code, and is based on the jj coupling scheme. Further relativistic corrections arising from the Breit interaction and QED effects (vacuum polarization and Lamb shift) have also been included in the same way as in the original version described in [21] and [25]. Additionally, we have used the option of *extended average level* (EAL), in which a weighted (proportional to $2j+1$) trace of the Hamiltonian matrix is minimized. This produces a compromise set of orbitals describing closely lying states with moderate accuracy. For our calculations of Ω , we have adopted the *Dirac Atomic R-matrix Code* (DARC) of P H Norrington and I P Grant (<http://web.am.qub.ac.uk/DARC/>). However, the code does not include the Breit and QED corrections, and hence the target energies obtained are slightly different (and comparatively less accurate) than from GRASP. Finally, for comparison purposes we have performed parallel calculations with the *Flexible Atomic Code* (FAC) of Gu [26], available from the website <http://sprg.ssl.berkeley.edu/~mfgu/fac/>. This is also a fully relativistic code which provides a variety of atomic parameters, and (generally) yields results for energy levels and radiative rates comparable to GRASP – see, for example, [18] and [27], and references therein. However, the differences in collision strengths and subsequently in effective collision strengths between FAC and DARC can be large, particularly for forbidden transitions, as demonstrated in our earlier papers [11]–[20], and also discussed below in sections 5 and 6. Hence results from FAC will be helpful in assessing the accuracy of our energy levels and radiative rates, and in estimating the contribution of resonances to effective collision strengths, included in calculations with DARC but not in FAC.

2 Energy levels

The $1s^2$, $1s2\ell$, $1s3\ell$, $1s4\ell$ and $1s5\ell$ configurations of He-like ions give rise to the lowest 49 levels listed in Table 1 (a–e), in which we compare our level energies with GRASP (obtained *without* and *with* the inclusion of Breit and QED effects) with the critically evaluated data compiled by NIST. Also included in these tables are our results obtained from the FAC code (FAC1), including the same CI (configuration interaction) as in GRASP. Our level energies obtained without the Breit and QED effects (GRASP1) are consistently higher than the NIST values by up to ~ 1.7 Ryd, similar to the effect observed for other He-like ions [11]–[20]. However, the orderings are nearly the same as those of NIST. The inclusion of Breit and QED effects (GRASP2) lowers the energies by a maximum of ~ 1.9 Ryd, depending on the ion. As expected, the contribution of Breit and QED effects increases with increasing Z , but our GRASP2 energies are lower than the NIST listings by up to ~ 0.4 Ryd, depending on the ion. In addition, the orderings have slightly altered in a few instances, see for example the 4f and 5f levels. However, the energy differences between these swapped levels are very small. It may be noted that NIST compilations are mostly based on a variety of theoretical works resulting in small differences with our listed energies. Our FAC1 level energies are consistently higher by up to 0.2 Ryd than the GRASP2 results, for all ions, and hence are comparatively in better agreement with the NIST listings. The level orderings from FAC1 are also in general agreement with the calculations from GRASP, but differ in some instances, particularly for the $n = 5$ levels. This is mainly because the non-degeneracy among the levels of the $n = 5$ configurations is very small. A further inclusion of the $1s6\ell$ configurations, labelled FAC2 calculations in Table 1 (a–e), makes no appreciable difference either in the magnitude or orderings of the levels.

Finally, in Table 1 (a–e) we also list the energies of Whiteford *et al* [28], which are obtained with the *AutoStructure* (AS) code of Badnell [29], and are available at the APAP (Atomic Processes for Astrophysical Plasmas) website: http://amdpp.phys.strath.ac.uk/UK_APAP/. The AS energies are higher by up to ~ 2 Ryd, depending on the ion, than the corresponding reference values from NIST and our results from the FAC and GRASP codes. Differences between the NIST and our theoretical energy levels with the latter calculations increase with increasing Z , and are due to the higher-order relativistic effects being neglected in the AS calculations. More importantly, the level orderings are slightly different, particularly for levels 42 and higher, and the AS energies for some of the levels of the 5g configuration are non-degenerate. However, the energy differences among the levels of a configuration are very small, as noted above. To conclude, we may state that overall there is general agreement between our calculations with the FAC and GRASP codes for the energy levels of the He-like ions considered here, and there is no major discrepancy with the NIST listings. However, the NIST energies are not available for some levels, particularly of the $n = 5$ configurations, for which our energy levels either from the GRASP2 or FAC1 calculations should be adopted in modelling applications. For the remaining levels, the critically compiled listings of NIST may be preferred.

3 Radiative rates

The absorption oscillator strength (f_{ij}) and radiative rate A_{ji} (in s^{-1}) for a transition $i \rightarrow j$ are related by the following expression:

$$f_{ij} = \frac{mc}{8\pi^2 e^2} \lambda_{ji}^2 \frac{\omega_j}{\omega_i} A_{ji} = 1.49 \times 10^{-16} \lambda_{ji}^2 (\omega_j/\omega_i) A_{ji} \quad (1)$$

where m and e are the electron mass and charge, respectively, c is the velocity of light, λ_{ji} is the transition energy/wavelength in \AA , and ω_i and ω_j are the statistical weights of the lower (i) and upper (j) levels, respectively. Similarly, the oscillator strength f_{ij} (dimensionless) and the line strength S (in atomic unit, 1 a.u. = $6.460 \times 10^{-36} \text{ cm}^2 \text{ esu}^2$) are related by the standard equations given below.

For the electric dipole (E1) transitions

$$A_{ji} = \frac{2.0261 \times 10^{18}}{\omega_j \lambda_{ji}^3} S^{\text{E1}} \quad \text{and} \quad f_{ij} = \frac{303.75}{\lambda_{ji} \omega_i} S^{\text{E1}}, \quad (2)$$

for the magnetic dipole (M1) transitions

$$A_{ji} = \frac{2.6974 \times 10^{13}}{\omega_j \lambda_{ji}^3} S^{\text{M1}} \quad \text{and} \quad f_{ij} = \frac{4.044 \times 10^{-3}}{\lambda_{ji} \omega_i} S^{\text{M1}}, \quad (3)$$

for the electric quadrupole (E2) transitions

$$A_{ji} = \frac{1.1199 \times 10^{18}}{\omega_j \lambda_{ji}^5} S^{\text{E2}} \quad \text{and} \quad f_{ij} = \frac{167.89}{\lambda_{ji}^3 \omega_i} S^{\text{E2}}, \quad (4)$$

and for the magnetic quadrupole (M2) transitions

$$A_{ji} = \frac{1.4910 \times 10^{13}}{\omega_j \lambda_{ji}^5} S^{\text{M2}} \quad \text{and} \quad f_{ij} = \frac{2.236 \times 10^{-3}}{\lambda_{ji}^3 \omega_i} S^{\text{M2}}. \quad (5)$$

In Table 2 (a–e) we present transition energies/wavelengths (λ , in Å), radiative rates (A_{ji} , in s^{-1}), oscillator strengths (f_{ij} , dimensionless), and line strengths (S , in a.u.), in length form (Babushkin gauge) only, for all 336 electric dipole (E1) transitions among the 49 levels of the He-like ions considered here. The *indices* used to represent the lower and upper levels of a transition have already been defined in Table 1 (a–e). Similarly, there are 391 electric quadrupole (E2), 316 magnetic dipole (M1), and 410 magnetic quadrupole (M2) transitions among the 49 levels. However, for these transitions only the A -values are listed in Table 2, and the corresponding results for the f - or S - values can be easily obtained using Eqs. (1–5).

As stated earlier, no other A -values are available in the literature with which to compare our results. Therefore, we have performed another calculation with the FAC code of Gu [26]. For all strong transitions ($f \geq 0.01$), the A -values from GRASP and FAC, in the Babushkin gauge, agree to better than 10% for the five ions. Furthermore, for a majority of the strong E1 transitions ($f \geq 0.01$) the length and velocity (Coulomb gauge) forms in our GRASP calculations agree within 10%. However, the differences are larger for a few transitions, which are among the degenerate levels of a configuration, such as 10–11 ($f \sim 1.4 \times 10^{-4}$), 24–25 ($f \sim 8.5 \times 10^{-6}$) and 27–29 ($f \sim 1.9 \times 10^{-7}$) in Ga XXX. This is because their transition energy (ΔE) is very small and hence a slight variation in ΔE has a considerable effect on the A -values. For a few such weaker transitions ($f < 10^{-3}$) the two forms of the f - value differ by orders of magnitude, for all ions. Finally, as for the energy levels the effect of additional CI is negligible on the A - values, as results for all transitions agree within 10% with those obtained with the inclusion of the $n = 6$ configurations. Therefore, for almost all strong E1 transitions our radiative rates should be accurate to better than 10%. However, for a few weaker transitions the accuracy is comparatively lower.

4 Lifetimes

The lifetime τ for a level j is defined as follows:

$$\tau_j = \frac{1}{\sum_i A_{ji}}. \quad (6)$$

Since this is a measurable parameter, it provides a check on the accuracy of the calculations. Therefore, in Table 1 (a–e) we have also listed our calculated lifetimes, which include the contributions from four types of transitions, i.e. E1, E2, M1 and M2. Unfortunately to our knowledge no similar theoretical or experimental data are available with which to compare our results. However, based on the accuracy assessment of our A -values, we expect our lifetimes to have the same level of accuracy.

5 Collision strengths

Collision strengths (Ω) are related to the more commonly known collision cross section (σ_{ij} , πa_0^2) by the following relationship:

$$\Omega_{ij}(\text{E}) = k_i^2 \omega_i \sigma_{ij}(\text{E}) \quad (7)$$

where k_i^2 is the incident energy of the electron and ω_i is the statistical weight of the initial state. Results for collisional data are preferred in the form of Ω because it is a symmetric and dimensionless quantity.

For the computation of collision strengths Ω , we have employed the *Dirac atomic R-matrix code* (DARC), which includes the relativistic effects in a systematic way, in both the target description and the scattering model. It is based on the jj coupling scheme, and uses the Dirac-Coulomb Hamiltonian in the R -matrix approach. The R -matrix radii adopted for Ga XXX, Ge XXXI, As XXXII, Se XXXIII and Br XXXIV are 2.88, 2.72, 2.56, 2.40 and 2.24 au, respectively. For all five ions, 60 continuum orbitals have been included for each channel angular momentum in the expansion of the wavefunction, allowing us to compute Ω up to an energy of 2150, 2350, 2650, 3000 and 3400 Ryd for Ga XXX, Ge XXXI, As XXXII, Se XXXIII and Br XXXIV, respectively. These energy ranges are sufficient to calculate values of effective collision strengths Υ (see section 6) up to $T_e = 10^8$ K, appropriate for applications to the modelling of high temperature laboratory plasmas. The maximum number of channels for a partial wave is 217, and the corresponding size of the Hamiltonian matrix is 13 076. To obtain convergence of Ω for all transitions and at all energies, we have included all partial waves with angular momentum $J \leq 40.5$, although a larger number would have been preferable for the convergence of some allowed transitions, especially at higher energies. However, to account for higher neglected partial waves, we have included a top-up, based on the Coulomb-Bethe approximation [30] for allowed transitions and geometric series for others.

For illustration, in Figs. 1–3 we show the variation of Ω with angular momentum J for three transitions of Ga XXX, namely 2–5 ($1s2s\ ^3S_1 - 1s2p\ ^3P_1^o$), 2–11 ($1s2s\ ^3S_1 - 1s3p\ ^3P_1^o$), and 9–12 ($1s3p\ ^3P_0^o - 1s3p\ ^3P_2^o$), and at three energies of 1000, 1400 and 1800 Ryd. Values of Ω have fully converged for all *resonance* transitions (including the allowed ones), plus a majority of the allowed transitions among the higher excited levels, as shown in Fig. 2 for the 2–11 transition. It is also clear from Fig. 2 that the need to include a larger range of partial waves increases with increasing energy. However, values of Ω have not converged for those allowed transitions whose ΔE is very small (mainly within the same n complex), as shown for the 2–5 transition in Fig. 1. Similarly, values of Ω have (almost) converged for all forbidden transitions, including those whose ΔE is very small, such as the 9–12 transition shown in Fig. 3. Therefore, for the allowed transitions within the same n complex, our wide range of partial waves is not sufficient for the convergence of Ω , for which a top-up has been included as mentioned above, and has been found to be appreciable.

In Table 3 (a–e) we list our values of Ω for resonance transitions of Ga XXX, Ge XXXI, As XXXII, Se XXXIII and Br XXXIV at energies *above* thresholds. The indices used to represent the levels of a transition have already been defined in Table 1 (a–e). Unfortunately, no similar data are available for comparison purposes as already stated in section 1. Therefore, to assess the accuracy of Ω , we have performed another calculation using the FAC code of Gu [26]. This code is also fully relativistic, and is based on the well-known and widely-used *distorted-wave* (DW) method. Furthermore, the same CI is included in FAC as in the calculations from DARC. Therefore, also included in Table 3 (a–e) for comparison purposes are the Ω values from FAC at a single *excited* energy E_j , which corresponds to an incident energy of $\sim 2000, 2100, 2300, 2400$ and 2600 Ryd for Ga XXX, Ge XXXI, As XXXII, Se XXXIII and Br XXXIV, respectively. For a majority of transitions the two sets of Ω generally agree well (within $\sim 20\%$). However, the differences are larger for a few (particularly weaker) transitions. For example, for 70% of the Ga XXX transitions, the values of Ω agree to within 20% at an energy of 2000 Ryd, and the discrepancies for others are mostly within a factor of two, although for some transitions (such as: 19–49, 33–38/41/43/47/49), the differences are up to an order of magnitude. However, most of these transitions are weak ($\Omega \sim 10^{-6}$) and forbidden, i.e. the values of Ω have fully converged at *all* energies within our adopted range of partial waves in the calculations from the DARC code. For such weak transitions, values of Ω from the FAC code are not assessed to be accurate. The values of Ω are higher from DARC for some transitions, whereas for others are higher from the FAC code. Additionally, for a few transitions, such as 18–28/29/30/31, values of Ω from the FAC code show an anomalous behaviour towards the higher end of the energy range. This problem is common for all ions and examples can be seen in Fig. 6 of Aggarwal and Keenan [16] – [17]. The sudden anomalous behaviour in values of Ω from the FAC code is also responsible for

the differences noted above for some of the transitions. Such anomalies for some transitions (both allowed and forbidden) from the FAC calculations arise primarily because of the interpolation and extrapolation techniques employed in the code, which is designed to generate a large amount of atomic data in a comparatively very short period of time, and without too large loss of accuracy. Similarly, some differences in Ω are expected because the DW method generally overestimates the results due to the exclusion of channel coupling. Such discrepancies, for a similar number of transitions, have also been noted for Ge XXXI, As XXXII, Se XXXIII and Br XXXIV.

As a further comparison between the DARC and FAC values of Ω , in Fig. 4 we show the variation of Ω with energy for three *allowed* transitions among the excited levels of Ga XXX, namely 5–14 (1s2p $^3P_1^o$ - 1s3d 3D_2), 12–26 (1s3p $^3P_2^o$ - 1s4d 3D_3), and 15–27 (1s3p $^1P_1^o$ - 1s4d 1D_2). Also included in this figure are the corresponding results obtained with the FAC code. For many transitions there are no discrepancies between the f -values obtained with the two different codes (GRASP and FAC), and therefore the values of Ω also agree to better than 20%. However, the values of Ω obtained with FAC are underestimated in comparison to our calculations with DARC, particularly towards the lower end of the energy range. Similar comparisons between the two calculations with DARC and FAC are shown in Fig. 5 for three *forbidden* transitions of Ga XXX, namely 2–8 (1s2s 3S_1 - 1s3s 3S_1), 2–16 (1s2s 3S_1 - 1s3d 3D_3), and 6–12 (1s2p $^3P_2^o$ - 1s3p $^3P_2^o$). As in the case of allowed transitions, for these forbidden ones the agreement between the two calculations improves considerably with increasing energy, but the differences are significant towards the lower end of the energy range, as Ω from FAC are underestimated. These anomalies are due to the interpolation and extrapolation techniques employed in the FAC code, as stated above. Therefore, on the basis of these and other comparisons discussed above, collision strengths from the FAC code are not assessed to be very accurate, over the entire energy range, for a majority of transitions for the above named five He-like ions. However, we do not see any apparent deficiency in our DARC calculations for Ω , and estimate our results to be accurate to better than 20% for a majority of the (strong) transitions.

6 Effective collision strengths

Excitation rates, in addition to energy levels and radiative rates, are required for plasma modelling, and are determined from the collision strengths (Ω). Since the threshold energy region is dominated by numerous closed-channel (Feshbach) resonances, values of Ω need to be calculated in a fine energy mesh to accurately account for their contribution. Furthermore, in a plasma electrons have a wide distribution of velocities, and therefore values of Ω are generally averaged over a *Maxwellian* distribution as follows:

$$\Upsilon(T_e) = \int_0^\infty \Omega(E) \exp(-E_j/kT_e) d(E_j/kT_e), \quad (8)$$

where k is Boltzmann constant, T_e is electron temperature in K, and E_j is the electron energy with respect to the final (excited) state. Once the value of Υ is known the corresponding results for the excitation $q(i, j)$ and de-excitation $q(j, i)$ rates can be easily obtained from the following equations:

$$q(i, j) = \frac{8.63 \times 10^{-6}}{\omega_i T_e^{1/2}} \Upsilon \exp(-E_{ij}/kT_e) \quad \text{cm}^3 \text{s}^{-1} \quad (9)$$

and

$$q(j, i) = \frac{8.63 \times 10^{-6}}{\omega_j T_e^{1/2}} \Upsilon \quad \text{cm}^3 \text{s}^{-1}, \quad (10)$$

where ω_i and ω_j are the statistical weights of the initial (i) and final (j) states, respectively, and E_{ij} is the transition energy. The contribution of resonances may enhance the values of Υ over those of the background collision strengths (Ω_B), especially for the forbidden transitions, by up to an order of magnitude (or even more) depending on the transition, and particularly at low temperatures. Similarly, values of Ω need to be

calculated over a wide energy range (above thresholds) in order to obtain convergence of the integral in Eq. (8), as demonstrated in Fig. 7 of Aggarwal and Keenan [31].

To delineate resonances, we have performed our calculations of Ω at up to $\sim 127\,500$ energies in the thresholds region, depending on the ion. Close to thresholds (~ 0.1 Ryd above a threshold) the energy mesh is 0.001 Ryd, and away from thresholds is 0.002 Ryd. Thus care has been taken to include as many resonances as possible, and with as fine a resolution as is computationally feasible. The density and importance of resonances can be appreciated from Figs. 6–9, where we plot Ω as a function of energy in the thresholds region for the four most important transitions of He-like ions, namely 1–2 (z : $1s^2\ ^1S_0 - 1s2s\ ^3S_1$), 1–5 (y : $1s^2\ ^1S_0 - 1s2p\ ^3P_1^o$), 1–6 (x : $1s^2\ ^1S_0 - 1s2p\ ^3P_2^o$), and 1–7 (w : $1s^2\ ^1S_0 - 1s2p\ ^1P_1^o$). Resonances shown in these figures are for transitions in Ga XXX, but similar dense resonances have been noted for all He-like ions. For some transitions, such as 1–2, 1–5 and 1–6, the resonances are dense, particularly at energies just above the thresholds, and are spread over a wide energy range of ~ 150 Ryd. These near-threshold resonances affect the values of Υ particularly towards the lower end of the temperature range.

Our calculated values of Υ are listed in Table 4 (a–e) over a wide temperature range up to 10^8 K, suitable for applications in a variety of plasmas. As stated in section 1, there are no other results available with which to compare. Therefore, we have also calculated values of Υ from our non-resonant Ω data obtained with the FAC code. These calculations are particularly helpful in providing an estimate of the importance of resonances in the determination of excitation rates. In Table 4 (a–e) we have included these results from FAC at the lowest and the highest calculated temperatures for Ga XXX, Ge XXXI, As XXXII, Se XXXIII and Br XXXIV. However, for discussion we focus solely on transitions in Ga XXX. At $T_e = 10^{6.4}$ K, our resonance-resolved values of Υ are higher by over 20% for about 37% of the transitions. Generally, the differences for a majority of the transitions are within a factor of two, but are up to a factor of five for a few. Furthermore, for a majority of transitions the Υ values from the DARC code are higher, partly due to the inclusion of resonances in the calculations with DARC but also because of the underestimation of Ω at lower energies in the FAC calculations, as demonstrated in Figs. 4 and 5 and discussed in section 5. In the case of the most important w , x , y , and z lines, resonances have significantly enhanced the values of Υ , by about a factor of 2.5, for the z (1–2: $1s^2\ ^1S_0 - 1s2s\ ^3S_1$) transition. A similar comparison at the highest temperature of our calculations, i.e. $10^{7.8}$ K, indicates that about 39% of the transitions in Ga XXX show differences of over 20% between the DARC and FAC values for Υ . These differences are generally within a factor of two, but are higher (up to an order of magnitude) for a few, such as: 18–28 (allowed transition) and 18–29/30/31 (forbidden). For all such transitions the FAC results are *higher*, mainly because of the sudden anomalies in the values of Ω , as discussed in section 5. Similar differences in Υ are noted for a comparable number of transitions in the other He-like ions, as shown in Table 4 (a–e).

Whiteford *et al* [28] have undertaken semi-relativistic calculations for Ar XVII and Fe XXV, using the standard R -matrix code of Berrington *et al* [32]. Recently they have placed their results for Υ for He-like ions up to $Z = 36$ on the APAP website: http://amdpp.phys.strath.ac.uk/UK_APAP/. In their calculations electron exchange was included for partial waves up to $J = 10.5$, but was neglected for higher J values. Furthermore, the calculations were performed in the LS coupling scheme and the corresponding results for Ω and subsequently Υ for fine-structure transitions obtained using their intermediate coupling frame transformation (ICFT) method. However, the data obtained by such procedures are generally comparable with our fully relativistic results from the DARC code, as has already been demonstrated in several papers – see for example, Liang and Badnell [33]. Furthermore, Whiteford *et al* included the effect of radiation damping. This can reduce the contribution of resonances to the determination of Υ for some transitions, such as $1s2p\ ^1P_1^o - 1s3s\ ^1S_0$, particularly towards the lower end of the temperature range (see their Fig. 4). However, at temperatures relevant to plasma modelling the effect is negligible. Radiation damping may be significant for highly charged ions, because radiative decay rates are large and compete with autoionisation rates [34]–[35]. However, similar R -matrix calculations performed by Delahaye *et al* [35] for several He-like ions up to $Z = 20$, with the inclusion of radiation damping, show that their contribution (i.e. reduction in values of Υ) is appreciable only at lower temperatures (below

10^6 K), which should not be important in plasma modelling applications for such highly ionised species. This has also been confirmed in calculations by Whiteford *et al* [28], who have shown that the resultant uncertainties in the excited level populations for the important w , x , y and z lines of Ar XVII and Fe XXV, at appropriate temperatures and densities, are under 10%. Finally, in a comparatively more recent calculations for Fe XXV and Kr XXXV using the the DARC code, Griffin and Ballance [36] have concluded that the damping effect on excitation to the vast majority of levels for both ions is small. Specifically, the differences between the two sets of calculations (with and without damping) when averaged over six temperatures ranging from 1.25×10^6 to 3.12×10^8 K for the lowest 30 resonance transitions are only 4% for Fe XXV and 4.4% for Kr XXXV. Similarly, the corresponding differences for all 1176 transitions over a wider range of nine temperatures are only 1.1% and 1.3%, for the respective ions. These differences are much smaller than the errors introduced by other parameters, such as inadequacies of partial waves, configuration interaction, energy mesh, and inclusion of a limited energy range. We can therefore confidently conclude that radiation damping is not important for the He-like ions considered here.

We now compare our results of Υ with those of Whiteford *et al* [28], and for illustration focus only on transitions in Ga XXX. Differences between the two sets of results are quite significant (over 20%) for many transitions, and throughout the temperature range of the calculations. To be specific, at the lowest common temperature of 1.8×10^5 K, the two sets of Υ differ by over 20% for $\sim 35\%$ of the transitions. For a majority of transitions, these differences are within a factor of two, and for some our results are higher whereas for most the reverse is true. However, for a few transitions the differences are up to a factor of five, and for the ‘elastic’ transitions, such as: 14–16/17, 16–17, 23–24/26/27, and 24–26/27, the discrepancies are up to two orders of magnitude, with the Υ values of Whiteford *et al* being invariably higher. Most of these belong to the degenerate levels of a state/configuration, and hence have very small transition energies. To demonstrate the differences between the two calculations, in Fig. 10 we compare values of Υ for three transitions of Ga XXX, namely 14–16 ($1s3d \ ^3D_2 - 1s3d \ ^3D_3$), 16–17 ($1s3d \ ^3D_3 - 1s3d \ ^1D_2$), and 24–26 ($1s4d \ ^3D_2 - 1s4d \ ^3D_3$). The differences in the Υ values are *not* due to resonances, but arise from the limitation of the approach adopted by Whiteford *et al* [28], as recently discussed and demonstrated by Bautista *et al* [37]. Similar large discrepancies are also observed with the calculations of Whiteford *et al* [38] for transitions in Li-like ions, as discussed and demonstrated by Aggarwal and Keenan [39],[40]. The problem in the R -matrix code adopted by Whiteford *et al* [28],[38] has been identified and rectified by Liang and Badnell [33]. However, since the calculations of Whiteford *et al* [28],[38] were performed more than a decade ago, limitations in their data for He-like ions remain.

Differences between our data for Υ from DARC and those of Whiteford *et al* [28] are not confined to lower temperatures, but cover the entire range of temperatures. For example, at the highest common temperature of 4.5×10^7 K, the two sets of Υ differ by over 20% for $\sim 13\%$ of the transitions of Ga XXX. Hence, there is comparatively a better convergence of the results at higher temperatures, but the Υ values of Whiteford *et al* are invariably higher. The differences for most transitions are within a factor of two, but for some are up to an order of magnitude, such as: 19–43/45, 29–31 and 33–43/45, and all transitions with the lower levels $I \geq 46$. Most of these transitions are *forbidden* and Ω for these have *converged* within our adopted partial waves range, as discussed in section 5. To demonstrate the differences, in Fig. 11 we compare our results of Υ from DARC with those of Whiteford *et al* [28] for three transitions of Ga XXX, namely 46–48 ($1s5g \ ^3G_3 - 1s5g \ ^3G_5$), 47–48 ($1s5g \ ^3G_4 - 1s5g \ ^3G_5$) and 48–49 ($1s5g \ ^3G_5 - 1s5g \ ^1G_4$). Since the collision strengths of Whiteford *et al* are overestimated for many transitions, particularly at the lower energies, the corresponding results for Υ are affected throughout the entire temperature range. To conclude, we may state that the Υ results of Whiteford *et al* [28] for transitions in Ga XXX and other He-like ions should not be as accurate as those presented here.

7 Conclusions

In this paper we have presented results for energy levels and radiative rates for four types of transitions (E1, E2, M1 and M2) among the lowest 49 levels of Ga XXX, Ge XXXI, As XXXII, Se XXXIII and Br XXXIV belonging to the $n \leq 5$ configurations. Additionally, lifetimes for all the calculated levels have been reported, although unfortunately no other theoretical or experimental results are available with which to compare. Furthermore, based on a variety of comparisons among various calculations with the GRASP and FAC codes, our data for radiative rates, oscillator strengths, line strengths, and lifetimes are judged to be accurate to better than 10% for a majority of the strong transitions (levels). Similarly, the accuracy of our results for collision strengths and effective collision strengths is estimated to be better than 20% for most transitions. We have considered a large range of partial waves to achieve convergence of Ω at all energies, included a wide energy range to accurately calculate values of Υ up to $T_e = 10^8$ K, and resolved resonances in a fine energy mesh to account for their contributions. Hence we see no apparent deficiency in our reported results. However, the present data for effective collision strengths for transitions involving the levels of the $n = 5$ configurations may be improved slightly by the inclusion of the levels of the $n = 6$ configurations. We believe the present set of complete results for radiative and excitation rates for transitions in five He-like ions should be useful for the modelling of a variety of plasmas.

Acknowledgment

KMA is grateful to AWE Aldermaston for financial support.

References

- [1] Dere K P, Landi E, Young P R and Del Zanna G 2001 *Astrophys. J. Suppl.* **134** 331
- [2] Feldman U, Ralchenko Y and Landi E 2008 *Astrophys. J.* **684** 707
- [3] Bitter M, Hill K W, Sauthoff N R, Efthimion P C, Meservey E, Roney W, von Goeler S, Horton R, Goldman M and Stodieck W 1979 *Phys. Rev. Lett.* **43** 129
- [4] Bitter M, von Goeler S, Hill K W, Horton R, Johnson D, Roney W, Sauthoff N, Silver E and Stodieck W 1981 *Phys. Rev. Lett.* **47** 921
- [5] Bitter M, Hsuan H, Decaux V, Grek B, Hill K W, Hulse R, Kruegel L A, Johnson D, von Goeler S and Zarnstorff M 1991 *Phys. Rev. A* **44** 1796
- [6] Bautista M A and Kallman T R 2000 *Astrophys. J.* **544** 581
- [7] Phillips K J H, Rainnie J A, Harra L K, Dubau J, Keenan F P and Peacock N J 2004 *Astron. Astrophys.* **416** 765
- [8] Iaria R, Di salvo T, Robba N R, Burderi L, Lavagetto G and Riggio A 2005 *Astrophys. J.* **634** L161
- [9] Porquet D, Dubau J and Grosso N 2010 *Space Sci. Rev.* **157** 103
- [10] Winter H P 2007 *J. Phys. Conf. Series* **58** 33
- [11] Aggarwal K M and Keenan F P 2005 *Astron. Astrophys.* **441** 831
- [12] Aggarwal K M and Keenan F P 2008 *Astron. Astrophys.* **489** 1377
- [13] Aggarwal K M, Keenan F P and Heeter R F 2009 *Phys. Scr.* **80** 045301

- [14] Aggarwal K M and Keenan F P 2010 *Phys. Scr.* **82** 065302
- [15] Aggarwal K M, Kato T, Keenan F P and Murakami I 2011 *Phys. Scr.* **83** 015302
- [16] Aggarwal K M and Keenan F P 2012 *Phys. Scr.* **85** 025305
- [17] Aggarwal K M and Keenan F P 2012 *Phys. Scr.* **85** 025306
- [18] Aggarwal K M and Keenan F P 2012 *Phys. Scr.* **85** 065301
- [19] Aggarwal K M and Keenan F P 2012 *Phys. Scr.* **86** 000000
- [20] Aggarwal K M and Keenan F P 2012 *Phys. Scr.* **86** 035302
- [21] Grant I P, McKenzie B J, Norrington P H, Mayers D F and Pyper N C 1980 *Comput. Phys. Commun.* **21** 207
- [22] Dylla K G, Grant I P, Johnson C T, Parpia F A and Plummer E P 1989 *Comput. Phys. Commun.* **55** 425
- [23] Parpia F A, Fischer C F and Grant I P 1996 *Comput. Phys. Commun.* **94** 249
- [24] Jönsson P, He X, Fischer C F and Grant I P 2007 *Comput. Phys. Commun.* **177** 597
- [25] Grant I P 1974 *J. Phys.* **B7** 1458
- [26] Gu M F 2008 *Can. J. Phys.* **86** 675
- [27] Aggarwal K M, Tayal V, Gupta G P and Keenan F P 2007 *At. Data Nucl. Data Tables* **93** 615
- [28] Whiteford A D, Badnell N R, Ballance C P, O'Mullane M G, Summers H P and Thomas A L 2001 *J. Phys.* **B 34** 3179
- [29] Badnell N R 1997 *J. Phys.* **B 30** 1
- [30] Burgess A and Sheorey V B 1974 *J. Phys.* **B7** 2403
- [31] Aggarwal K M and Keenan F P 2008 *Eur. Phys. J.* **D 46** 205
- [32] Berrington K A, Eissner W B and Norrington P H 1995 *Comput. Phys. Commun.* **92** 290
- [33] Liang G Y and Badnell N R 2011 *Astron. Astrophys.* **528** A69
- [34] Gorczyca T W, Robicheaux F, Pindzola M S and Badnell N R 1995 *Phys. Rev.* **A52** 3852
- [35] Delahaye F, Pradhan A K and Zeippen C J 2006 *J. Phys.* **B39** 3465
- [36] Griffin D C and Ballance C P 2009 *J. Phys.* **B 42** 235201
- [37] Bautista M A, Ballance C P and Quinet P 2010 *Astrophys. J. Lett.* **718** L189
- [38] Whiteford A D, Badnell N R, Ballance C P, Loch S D, O'Mullane M G and Summers H P 2002 *J. Phys.* **B 35** 3729
- [39] Aggarwal K M and Keenan F P 2012 *At. Data Nucl. Data Tables* **98** 1003
- [40] Aggarwal K M and Keenan F P 2013 *At. Data Nucl. Data Tables* **99** 156

Figure 1. Partial collision strengths for the 2–5 transition of Ga XXX.

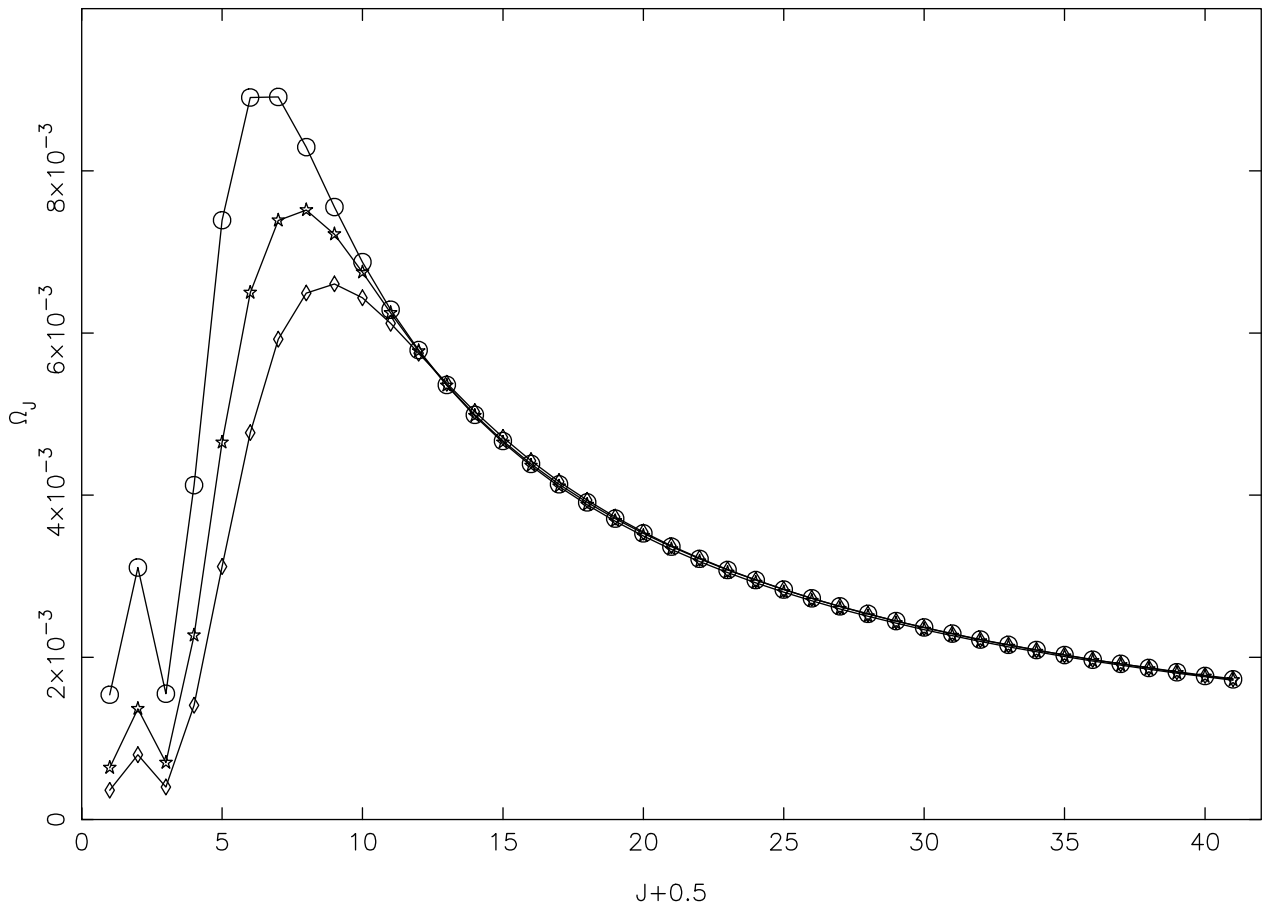


Figure 1: Partial collision strengths for the $1s2s\ ^3S_1 - 1s2p\ ^3P_1^o$ (2–5) transition of Ga XXX, at three energies of: 1000 Ryd (circles), 1400 Ryd (stars) and 1800 Ryd (diamonds).

Figure 2. Partial collision strengths for the 2–11 transition of Ga XXX.

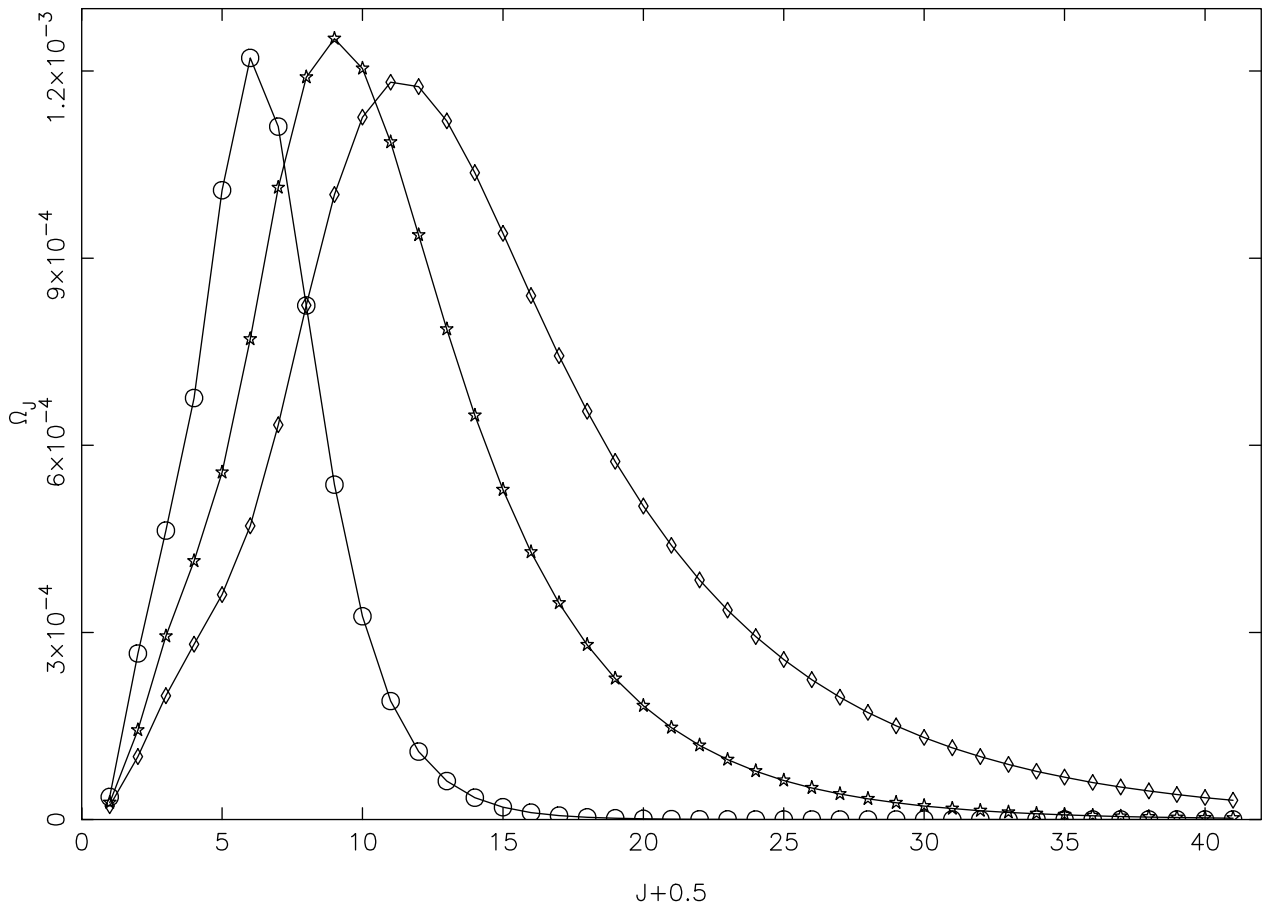


Figure 2: Partial collision strengths for the $1s2s\ ^3S_1 - 1s3p\ ^3P_1^o$ (2–11) transition of Ga XXX, at three energies of: 1000 Ryd (circles), 1400 Ryd (stars) and 1800 Ryd (diamonds).

Figure 3. Partial collision strengths for the 9–12 transition of Ga XXX.

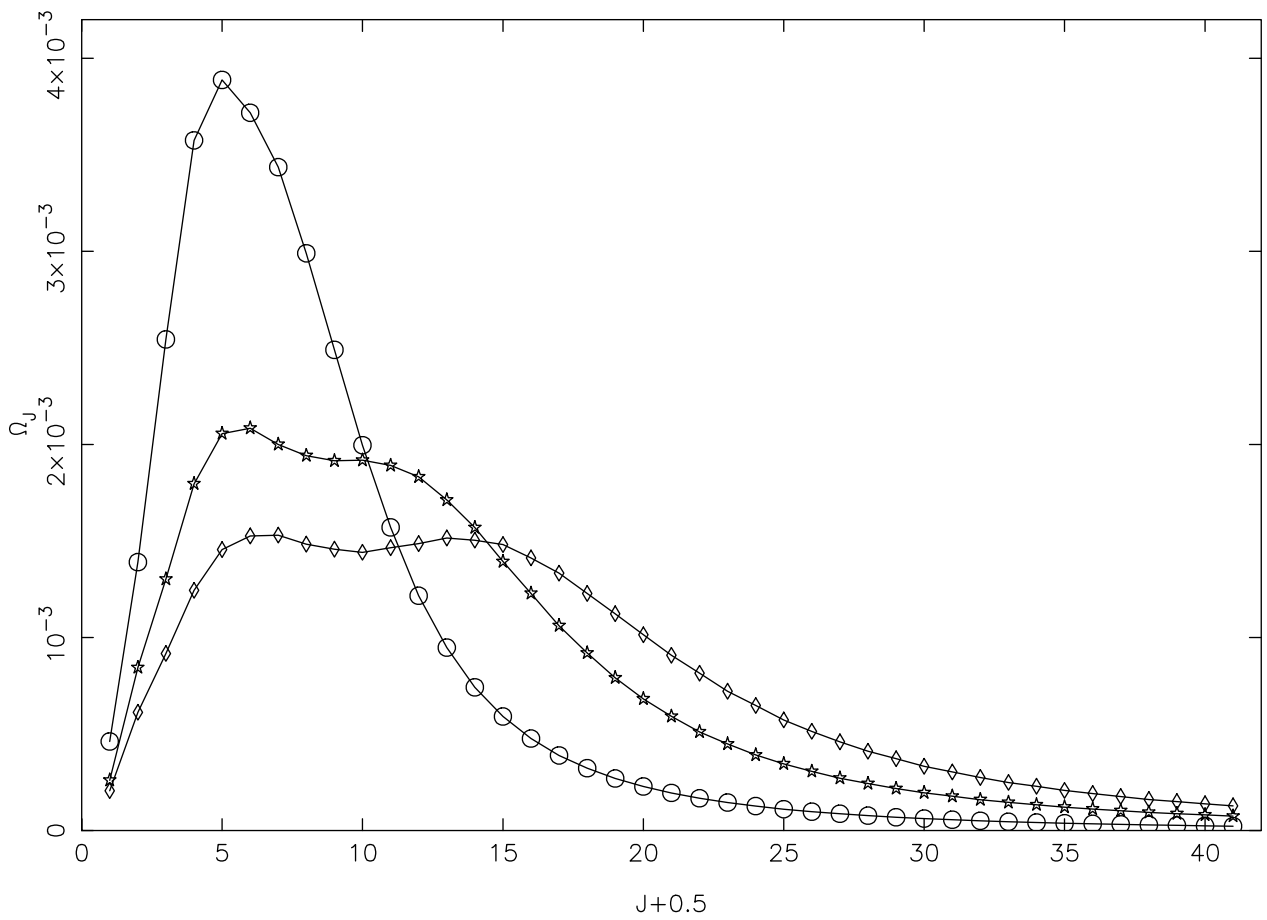


Figure 3: Partial collision strengths for the $1s3p\ ^3P_0^o - 1s3p\ ^3P_2^o$ (9–12) transition of Ga XXX, at three energies of: 1000 Ryd (circles), 1400 Ryd (stars) and 1800 Ryd (diamonds).

Figure 4. Comparison of collision strengths for the 5–14, 12–26 and 15–27 allowed transitions of Ga XXX.

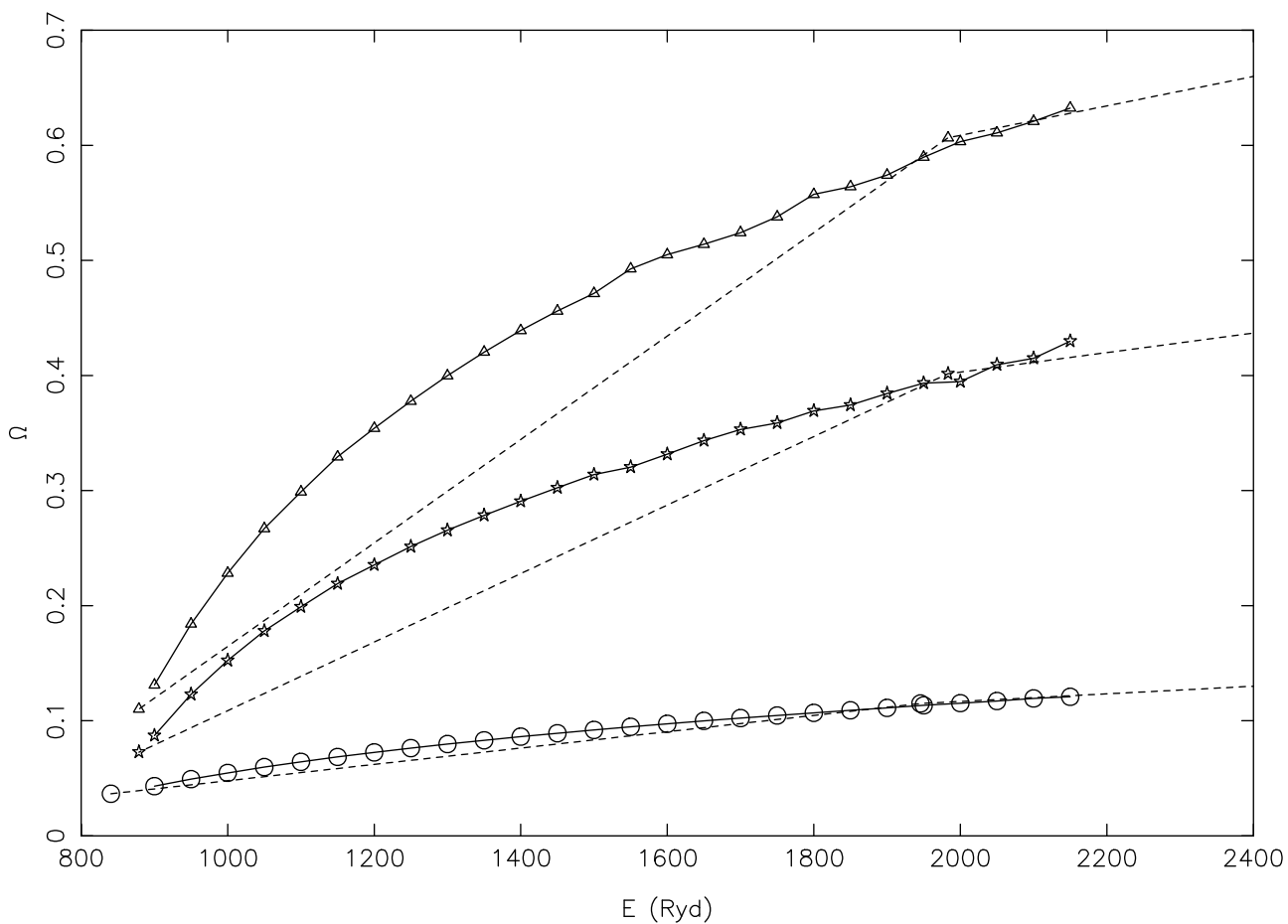


Figure 4: Comparison of collision strengths from our calculations from DARC (continuous curves) and FAC (broken curves) for the 5–14 (circles: $1s2p\ ^3P_1^o - 1s3d\ ^3D_2$), 12–26 (triangles: $1s3p\ ^3P_2^o - 1s4d\ ^3D_3$), and 15–27 (stars: $1s3p\ ^1P_1^o - 1s4d\ ^1D_2$) allowed transitions of Ga XXX.

Figure 5. Comparison of collision strengths for the 2–8, 2–16, and 6–12 forbidden transitions of Ga XXX.

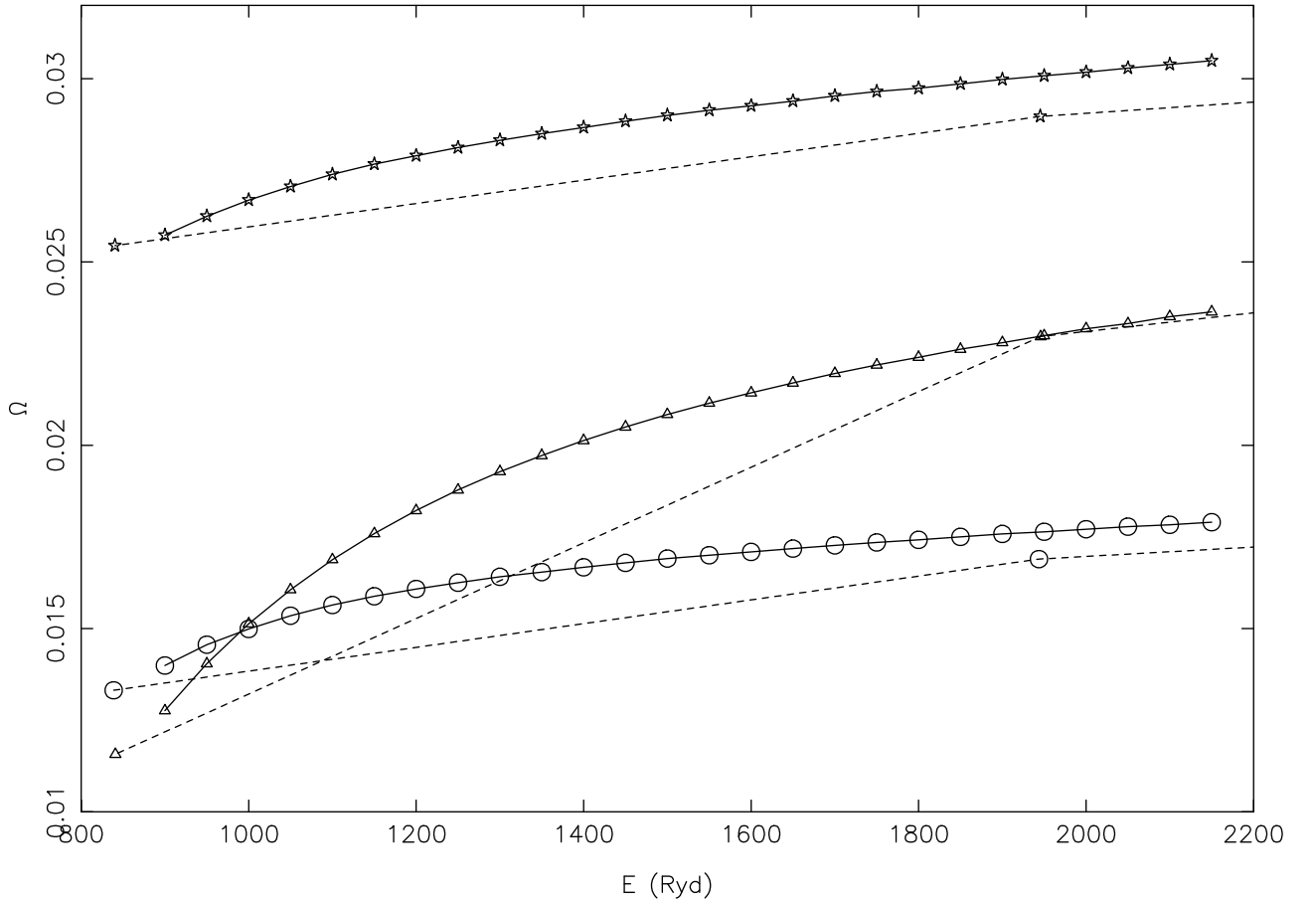


Figure 5: Comparison of collision strengths from our calculations from DARC (continuous curves) and FAC (broken curves) for the 2–8 (circles: $1s2s\ ^3S_1 - 1s3s\ ^3S_1$), 2–16 (triangles: $1s2s\ ^3S_1 - 1s3d\ ^3D_3$), and 6–12 (stars: $1s2p\ ^3P_2 - 1s3p\ ^3P_2$) forbidden transitions of Ga XXX.

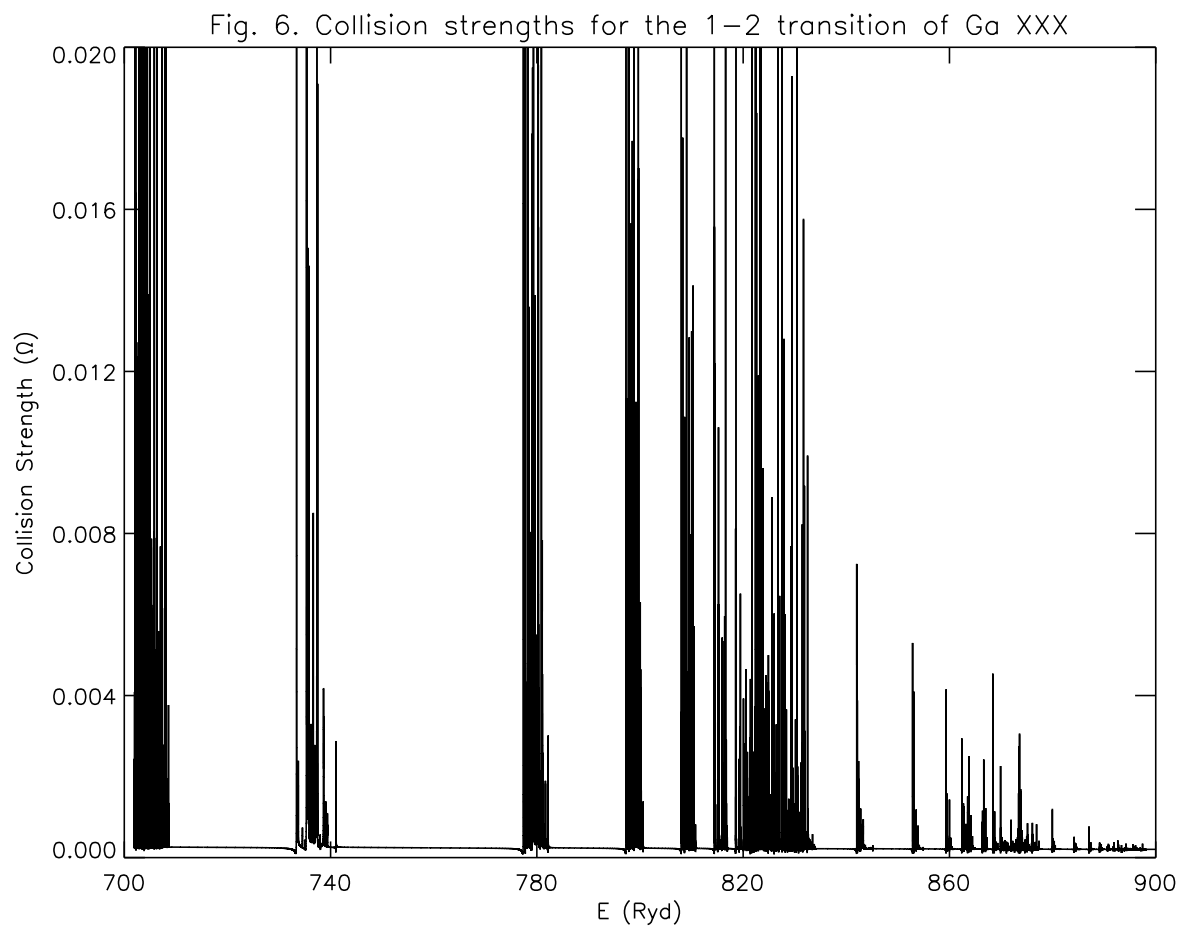


Figure 6: Collision strengths for the $1s^2\ ^1S_0 - 1s2s\ ^3S_1$ (1–2) transition of Ga XXX.

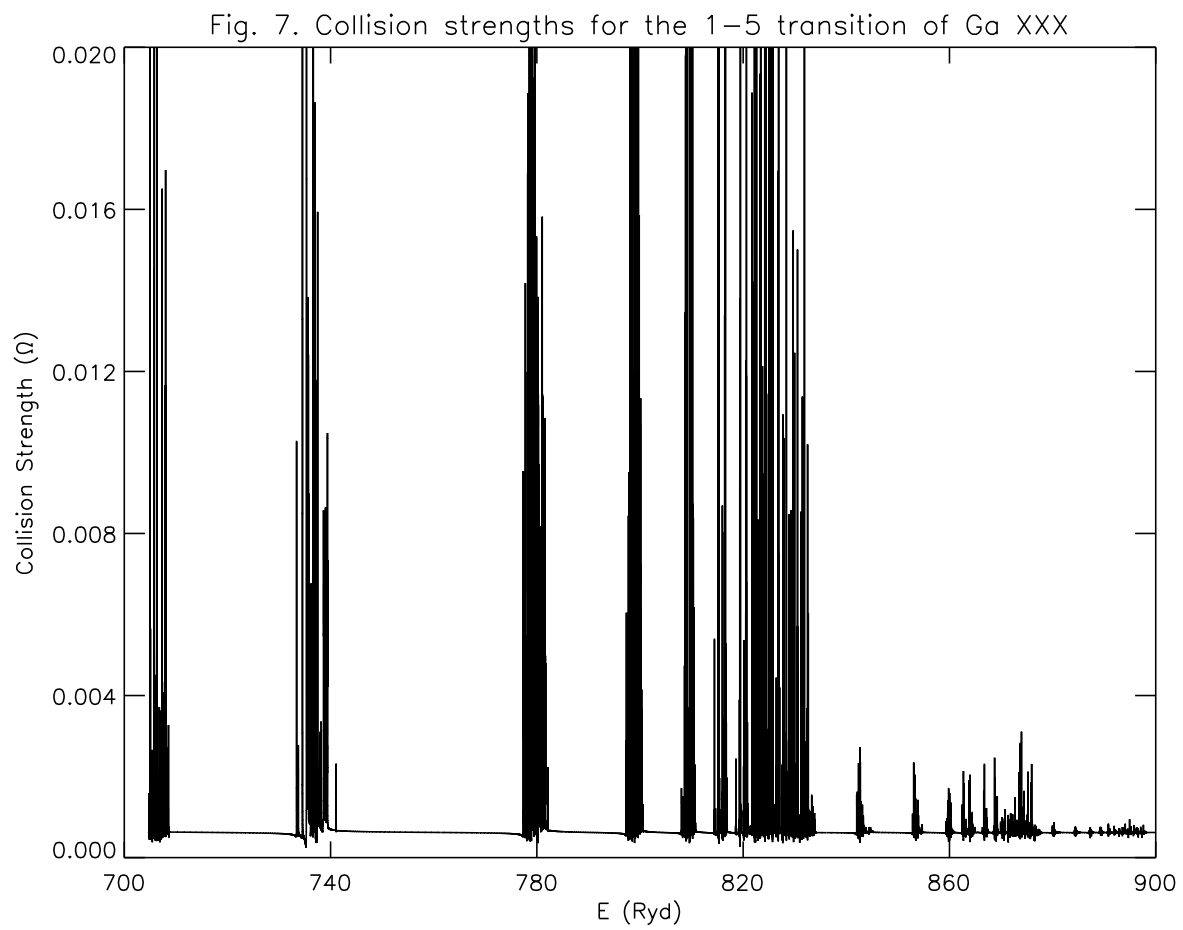


Figure 7: Collision strengths for the $1s^2\ ^1S_0 - 1s2p\ ^3P_1^o$ (1–5) transition of Ga XXX.

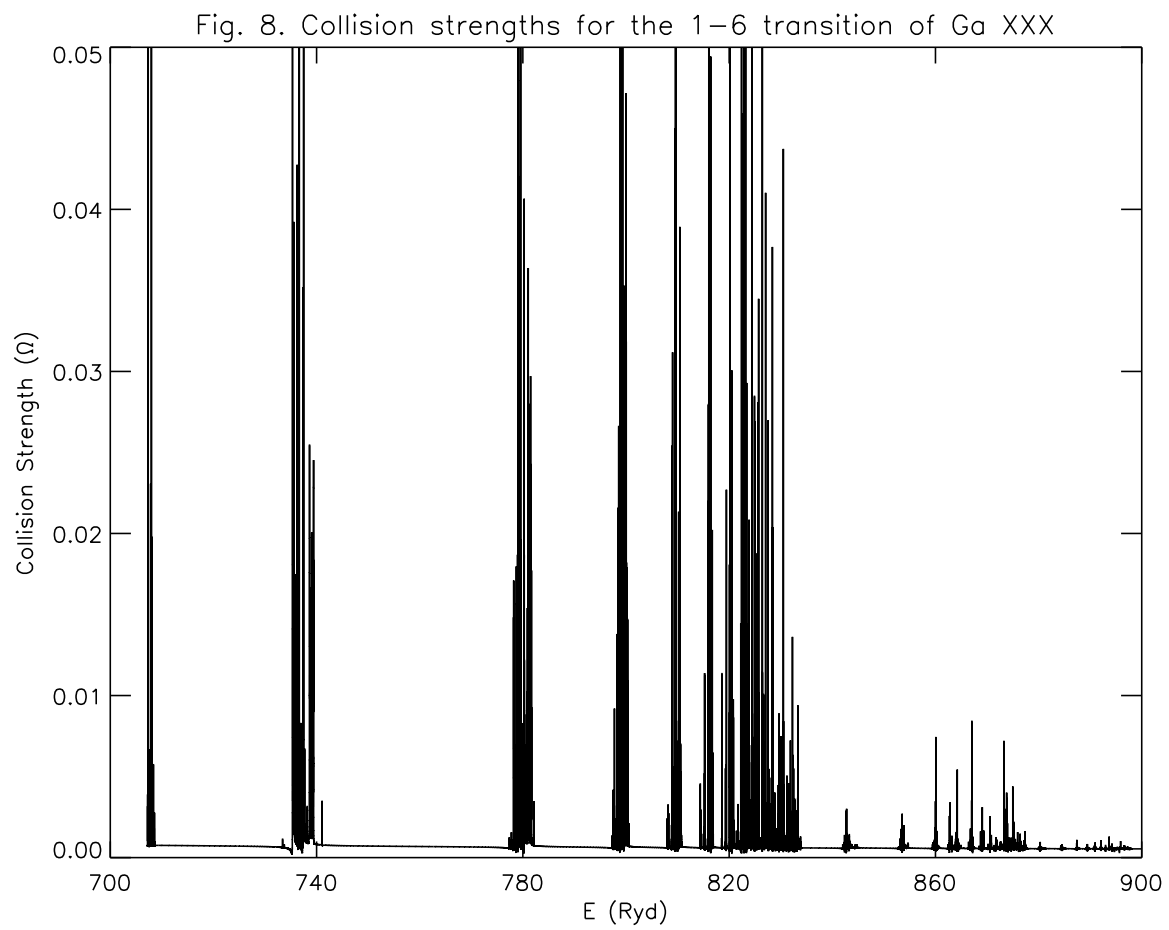


Figure 8: Collision strengths for the $1s^2\ ^1S_0 - 1s2p\ ^3P_2^o$ (1–6) transition of Ga XXX.

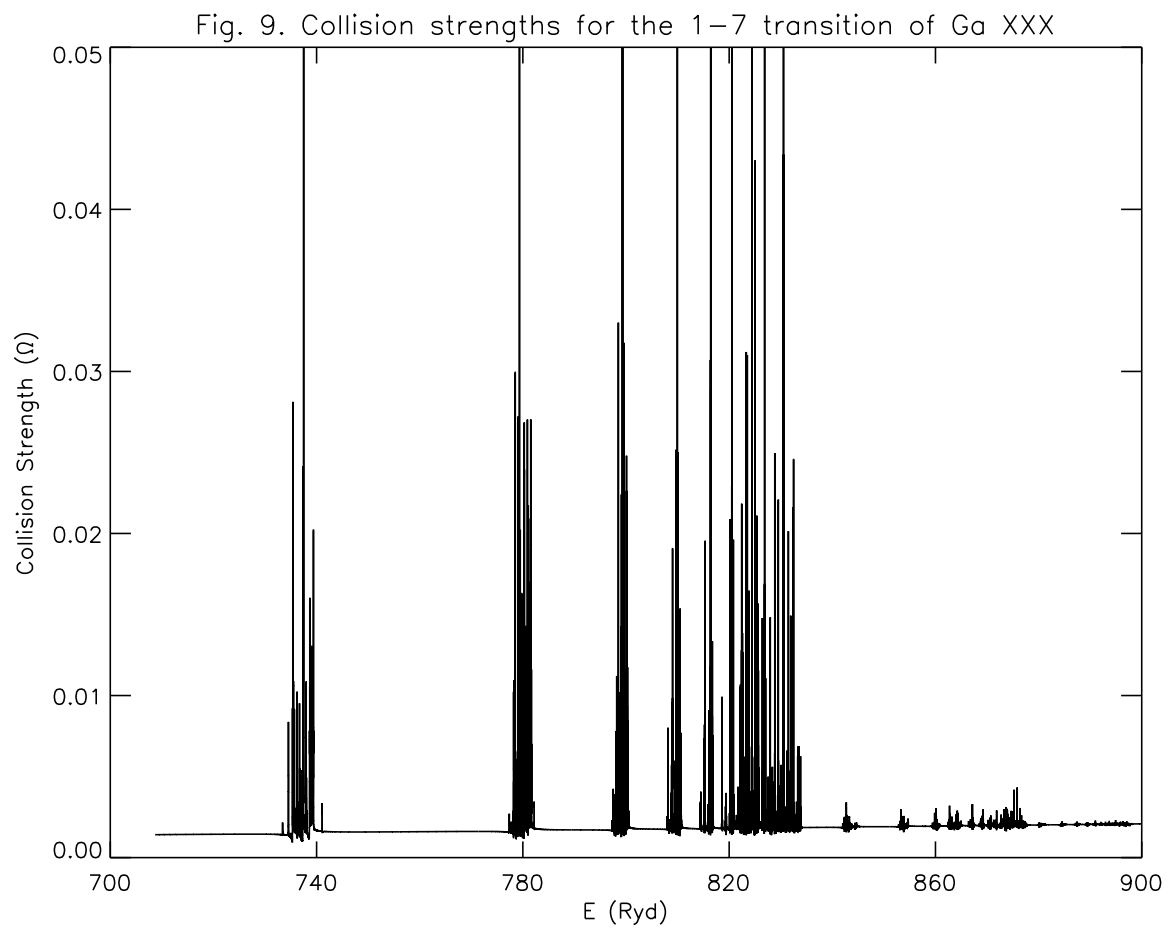


Figure 9: Collision strengths for the $1s^2\ ^1S_0 - 1s2p\ ^1P_1^o$ (1–7) transition of Ga XXX.

Figure 10. Comparison of effective collision strengths for the 14–16, 16–17 and 24–26 transitions of Ga XXX.

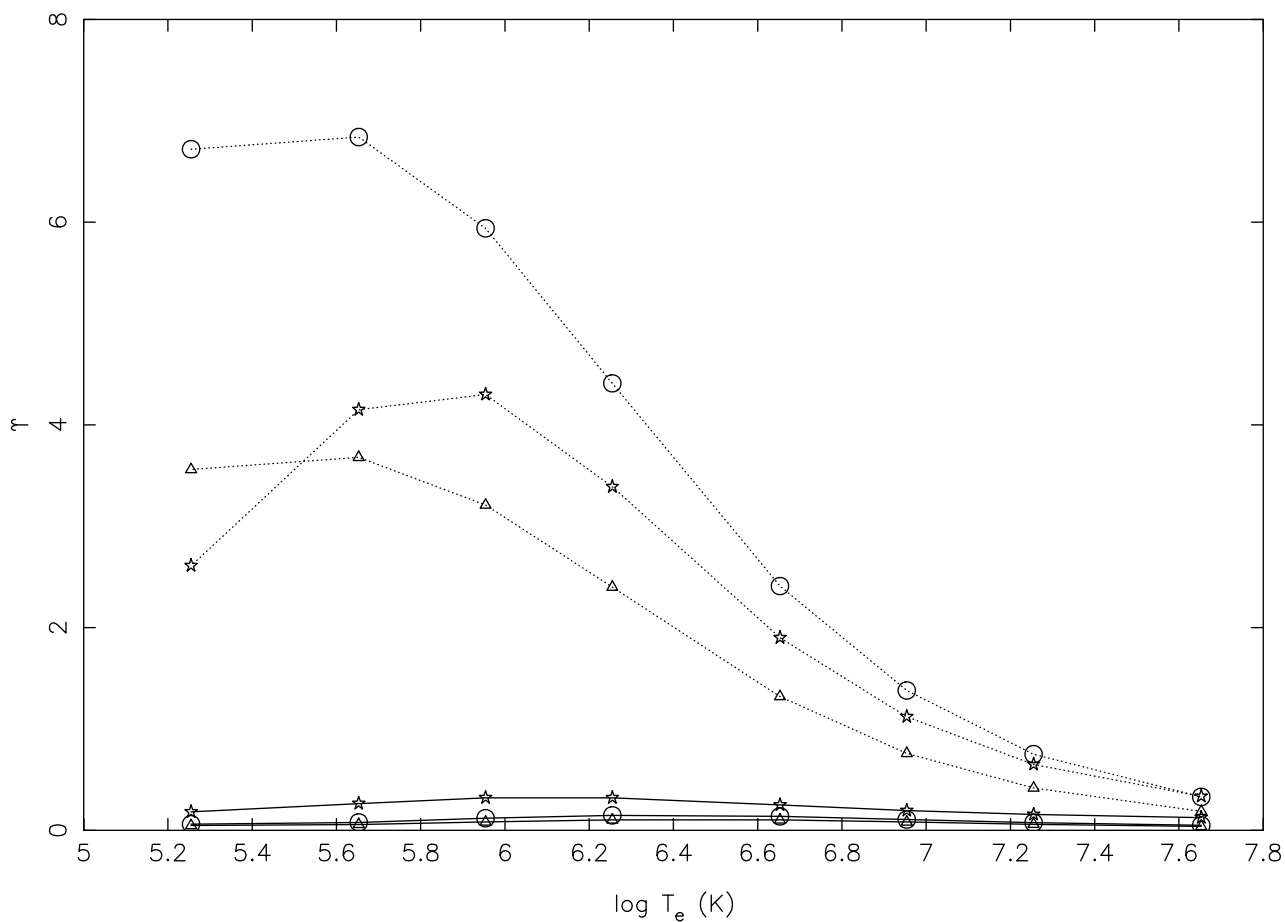


Figure 10: Comparison of effective collision strengths for the 14–16 (circles: $1s3d\ ^3D_2 - 1s3d\ ^3D_3$), 16–17 (triangles: $1s3d\ ^3D_3 - 1s3d\ ^1D_2$), and 24–26 (stars: $1s4d\ ^3D_2 - 1s4d\ ^3D_3$) transitions of Ga XXX. Continuous and dotted curves are from the present DARC and earlier *R*-matrix codes [28], respectively.

Figure 11. Comparison of effective collision strengths for the 46–48, 47–48, and 48–49 transitions of Ga XXX.

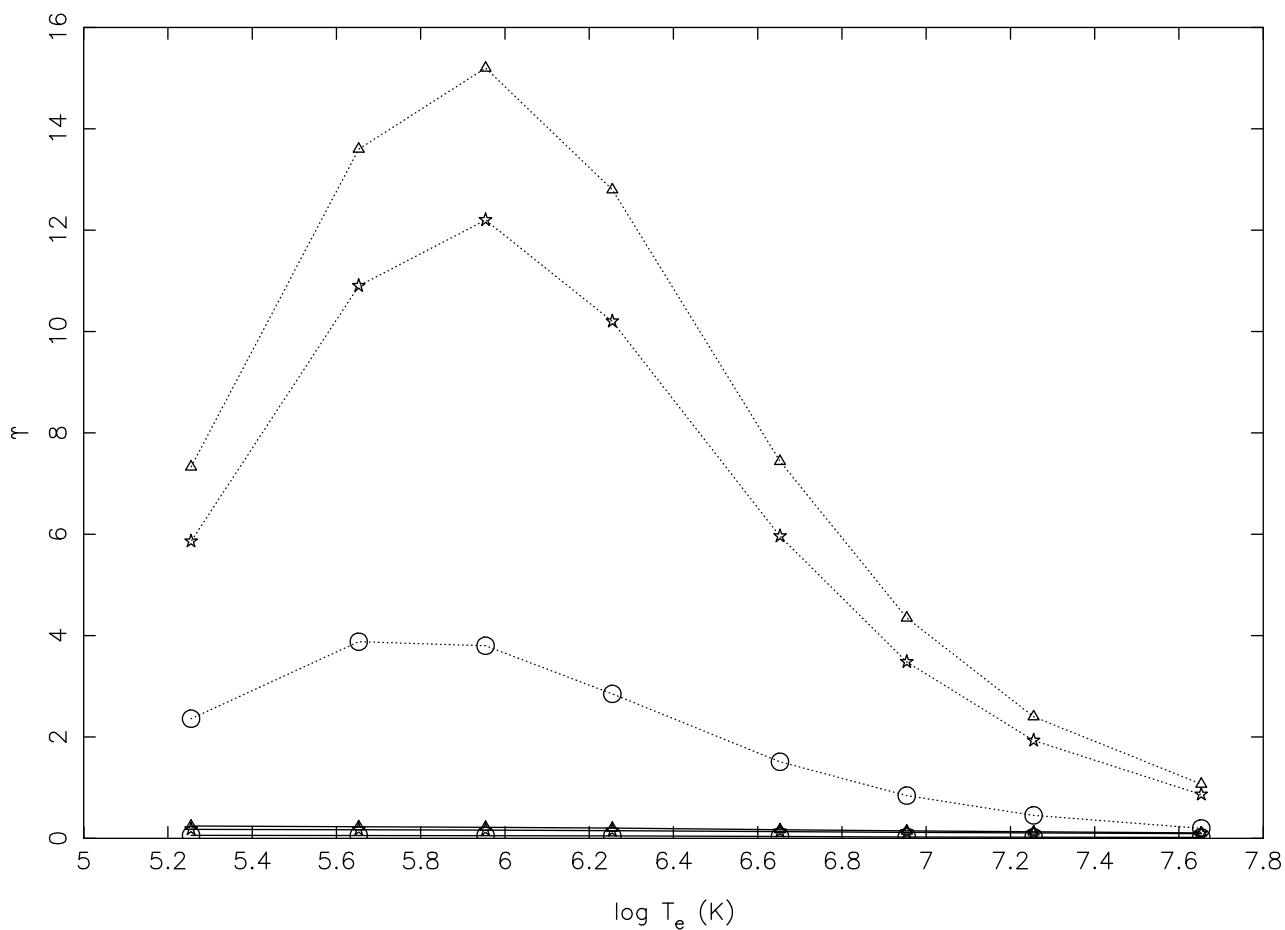


Figure 11: Comparison of effective collision strengths for the 46–48 (circles: $1s5g\ ^3G_3 - 1s5g\ ^3G_5$), 47–48 (triangles: $1s5g\ ^3G_4 - 1s5g\ ^3G_5$), and 48–49 (stars: $1s5g\ ^3G_5 - 1s5g\ ^1G_4$) transitions of Ga XXX. Continuous and dotted curves are from the present DARC and earlier *R*-matrix codes [28], respectively.

Table 1: a. Energy levels (in Ryd) of Ga XXX and their lifetimes (τ , s). $a \pm b \equiv a \times 10^{\pm b}$.

Index	Configuration/Level	NIST	GRASP1	GRASP2	FAC1	FAC2	AS	τ (s)
1	1s ² ¹ S ₀	0.00000	0.00000	0.00000	0.00000	0.00000	0.00000
2	1s2s ³ S ₁	700.86597	701.83875	700.59790	700.73132	700.73102	702.11621	8.137-10
3	1s2p ³ P ₀ ^o	703.52441	704.29773	703.26678	703.43005	703.42999	704.47528	2.070-09
4	1s2s ¹ S ₀	703.73382	704.60309	703.51764	703.66174	703.66138	704.94012	2.190-03
5	1s2p ³ P ₁ ^o	703.71860	704.72906	703.46155	703.63263	703.63251	704.91608	6.376-15
6	1s2p ³ P ₂ ^o	706.14166	707.17432	705.88123	706.04395	706.04382	707.36456	3.196-11
7	1s2p ¹ P ₁ ^o	707.66900	708.70074	707.42346	707.61078	707.61066	708.94946	1.123-15
8	1s3s ³ S ₁	830.87033	831.90155	830.60962	830.76263	830.76239	832.19769	1.617-13
9	1s3p ³ P ₀ ^o	831.60281	832.58154	831.34540	831.50067	831.50061	832.83984	5.362-14
10	1s3s ¹ S ₀	831.63510	832.63214	831.38556	831.53259	831.53241	832.90070	1.610-13
11	1s3p ³ P ₁ ^o	831.65690	832.70105	831.40076	831.55780	831.55774	832.95496	1.565-14
12	1s3p ³ P ₂ ^o	832.38076	833.43121	832.12354	832.27997	832.27979	833.66095	5.612-14
13	1s3d ³ D ₁	832.76987	833.80634	832.51001	832.65704	832.65704	834.03058	1.859-14
14	1s3d ³ D ₂	832.75629	833.81580	832.49683	832.64435	832.64435	834.04120	1.856-14
15	1s3p ¹ P ₁ ^o	832.79611	833.84375	832.54443	832.70276	832.70270	834.07385	3.797-15
16	1s3d ³ D ₃	833.01846	834.07513	832.75812	832.90497	832.90497	834.30786	1.892-14
17	1s3d ¹ D ₂	833.04750	834.09094	832.78772	832.93549	832.93549	834.32520	1.891-14
18	1s4s ³ S ₁	875.91260	876.96307	875.65991	875.80420	875.80396	877.24005	2.391-13
19	1s4p ³ P ₀ ^o	876.21880	877.24286	875.96198	876.09937	876.09924	877.50201	9.218-14
20	1s4s ¹ S ₀	876.22970	877.26007	875.97601	876.11591	876.11560	877.51215	2.235-13
21	1s4p ³ P ₁ ^o	876.24250	877.29211	875.98511	876.12311	876.12305	877.54706	3.362-14
22	1s4p ³ P ₂ ^o	876.54690	877.60040	876.29034	876.42865	876.42859	877.83502	9.582-14
23	1s4d ³ D ₁	876.71090	877.75427	876.44928	876.59924	876.59924	877.98401	4.323-14
24	1s4d ³ D ₂	876.70540	877.75928	876.44476	876.59497	876.59503	877.98950	4.314-14
25	1s4p ¹ P ₁ ^o	876.72270	877.76935	876.46326	876.60138	876.60126	877.99951	8.917-15
26	1s4d ³ D ₃	876.81570	877.86780	876.55408	876.70355	876.70355	878.09973	4.408-14
27	1s4d ¹ D ₂	876.82840	877.87640	876.56842	876.71838	876.71838	878.10712	4.397-14
28	1s4f ³ F ₂ ^o		877.87708	876.56818	876.70862	876.70874	878.10901	8.863-14
29	1s4f ³ F ₃ ^o		877.87720	876.56390	876.70441	876.70441	878.10699	8.861-14
30	1s4f ³ F ₄ ^o		877.93347	876.62061	876.76111	876.76111	878.16522	8.912-14
31	1s4f ¹ F ₃ ^o		877.93359	876.62390	876.76440	876.76440	878.16541	8.917-14
32	1s5s ³ S ₁	896.64490	897.69702	896.38977	896.52985	896.52966	897.96375	3.879-13
33	1s5p ³ P ₀ ^o		897.83850	896.54236	896.67773	896.67767	898.09497	1.594-13
34	1s5s ¹ S ₀	896.80620	897.84711	896.54980	896.68646	896.68610	898.09277	3.163-13
35	1s5p ³ P ₁ ^o	896.81250	897.86346	896.55420	896.68994	896.68976	898.11639	6.572-14
36	1s5p ³ P ₂ ^o	896.96840	898.02118	896.71039	896.84631	896.84613	898.25702	1.655-13
37	1s5d ³ D ₁		898.09888	896.79077	896.93866	896.93866	898.33087	8.334-14
38	1s5d ³ D ₂		898.10168	896.78870	896.93671	896.93671	898.33380	8.250-14
39	1s5p ¹ P ₁ ^o	897.05860	898.10681	896.79816	896.93341	896.93323	898.33759	1.838-14
40	1s5d ³ D ₃		898.15704	896.84442	896.99194	896.99194	898.38898	8.523-14
41	1s5d ¹ D ₂		898.16187	896.85217	897.00000	897.00000	898.39313	8.331-14
42	1s5f ³ F ₂ ^o		898.16223	896.85205	896.99219	896.99219	898.39404	1.710-13
43	1s5f ³ F ₃ ^o		898.16229	896.84991	896.99005	896.99005	898.39307	1.711-13
44	1s5f ³ F ₄ ^o		898.19110	896.87891	897.01904	897.01904	898.42267	1.721-13
45	1s5f ¹ F ₃ ^o		898.19122	896.88068	897.02075	897.02075	898.42273	1.722-13
46	1s5g ³ G ₃		898.19122	896.88049	897.02026	897.02026	898.42194	2.886-13
47	1s5g ³ G ₄		898.19122	896.87921	897.01904	897.01904	898.42194	2.886-13
48	1s5g ³ G ₅		898.20850 ₃	896.89661	897.03638	897.03638	898.43976	2.893-13

Table 1: b. Energy levels (in Ryd) of Ge XXXI and their lifetimes (τ , s). $a \pm b \equiv a \times 10^{\pm b}$.

Index	Configuration/Level	NIST	GRASP1	GRASP2	FAC1	FAC2	AS	τ (s)
1	1s ² 1S ₀	0.00000	0.00000	0.00000	0.00000	0.00000	0.00000
2	1s2s 3S ₁	748.31400	749.35278	747.98206	748.11768	748.11737	749.63153	5.872-10
3	1s2p 3P ₀ ^o	751.01363	751.90405	750.76447	750.93030	750.93018	752.07312	1.956-09
4	1s2s 1S ₀	751.22441	752.21918	751.01996	751.16595	751.16565	752.57642	1.711-03
5	1s2p 3P ₁ ^o	751.28783	752.36719	750.96320	751.13751	751.13733	752.54663	5.186-15
6	1s2p 3P ₂ ^o	754.00687	755.18738	753.75824	753.92365	753.92346	755.36475	2.482-11
7	1s2p 1P ₁ ^o	755.57598	756.74915	755.34058	755.52960	755.52948	756.98779	1.001-15
8	1s3s 3S ₁	887.14927	888.31311	886.88550	887.04102	887.04077	888.60968	1.413-13
9	1s3p 3P ₀ ^o	887.91273	889.01868	887.65234	887.81000	887.81000	889.27332	4.692-14
10	1s3s 1S ₀	887.94618	889.07037	887.69275	887.84222	887.84198	889.34064	1.408-13
11	1s3p 3P ₁ ^o	887.96780	889.14655	887.70868	887.86829	887.86823	889.39624	1.307-14
12	1s3p 3P ₂ ^o	888.80359	889.98871	888.54340	888.70233	888.70221	890.20734	4.926-14
13	1s3d 3D ₁	889.20682	890.37683	888.94409	889.09344	889.09344	890.58875	1.629-14
14	1s3d 3D ₂	889.19124	890.38666	888.92889	889.07880	889.07880	890.59973	1.626-14
15	1s3p 1P ₁ ^o	889.23052	890.41095	888.97571	889.13641	889.13635	890.62976	3.384-15
16	1s3d 3D ₃	889.49123	890.68347	889.22791	889.37708	889.37708	890.90466	1.660-14
17	1s3d 1D ₂	889.52231	890.69977	889.25946	889.40955	889.40955	890.92255	1.658-14
18	1s4s 3S ₁		936.45941	935.01917	935.16589	935.16571	936.73291	2.088-13
19	1s4p 3P ₀ ^o		936.74963	935.33398	935.47363	935.47357	937.00336	8.067-14
20	1s4s 1S ₀		936.76715	935.34802	935.49023	935.48993	937.01495	1.958-13
21	1s4p 3P ₁ ^o		936.80231	935.35748	935.49786	935.49774	937.05133	2.829-14
22	1s4p 3P ₂ ^o		937.15784	935.70990	935.85071	935.85052	937.38153	8.407-14
23	1s4d 3D ₁		937.31708	935.87476	936.02710	936.02710	937.53510	3.788-14
24	1s4d 3D ₂		937.32227	935.86945	936.02203	936.02203	937.54077	3.778-14
25	1s4p 1P ₁ ^o		937.33075	935.88757	936.02808	936.02795	937.54968	7.964-15
26	1s4d 3D ₃		937.44659	935.99463	936.14648	936.14648	937.66681	3.868-14
27	1s4d 1D ₂		937.45551	936.00989	936.16217	936.16217	937.67432	3.854-14
28	1s4f 3F ₂ ^o		937.45624	936.00952	936.15247	936.15247	937.67645	7.768-14
29	1s4f 3F ₃ ^o		937.45630	936.00482	936.14771	936.14771	937.67419	7.767-14
30	1s4f 3F ₄ ^o		937.52051	936.06946	936.21234	936.21234	937.74054	7.814-14
31	1s4f 1F ₃ ^o		937.52063	936.07312	936.21600	936.21600	937.74066	7.818-14
32	1s5s 3S ₁		958.61139	957.16663	957.30908	957.30884	958.87256	3.383-13
33	1s5p 3P ₀ ^o		958.75806	957.32556	957.46332	957.46326	959.00800	1.394-13
34	1s5s 1S ₀		958.76678	957.33301	957.47198	957.47162	959.00586	2.783-13
35	1s5p 3P ₁ ^o		958.78479	957.33759	957.47565	957.47552	959.03070	5.538-14
36	1s5p 3P ₂ ^o		958.96661	957.51794	957.65625	957.65607	959.19153	1.451-13
37	1s5d 3D ₁		959.04706	957.60132	957.75153	957.75153	959.26764	7.301-14
38	1s5d 3D ₂		959.04999	957.59882	957.74921	957.74921	959.27075	7.220-14
39	1s5p 1P ₁ ^o		959.05426	957.60809	957.74567	957.74554	959.27380	1.637-14
40	1s5d 3D ₃		959.11340	957.66266	957.81256	957.81256	959.33368	7.477-14
41	1s5d 1D ₂		959.11841	957.67090	957.82111	957.82111	959.33795	7.299-14
42	1s5f 3F ₂ ^o		959.11877	957.67078	957.81323	957.81323	959.33893	1.499-13
43	1s5f 3F ₃ ^o		959.11884	957.66833	957.81085	957.81085	959.33777	1.500-13
44	1s5f 3F ₄ ^o		959.15173	957.70148	957.84387	957.84387	959.37146	1.509-13
45	1s5f 1F ₃ ^o		959.15179	957.70337	957.84583	957.84583	959.37152	1.510-13
46	1s5g 3G ₃		959.15186	957.70312	957.84528	957.84528	959.37073	2.531-13
47	1s5g 3G ₄		959.15186	957.70172	957.84393	957.84393	959.37073	2.530-13
48	1s5g 3G ₅		959.17157 ₄	957.72156	957.86377	957.86377	959.39099	2.537-13

Table 1: c. Energy levels (in Ryd) of As XXXII and their lifetimes (τ , s). $a \pm b \equiv a \times 10^{\pm b}$.

Index	Configuration/Level	NIST	GRASP1	GRASP2	FAC1	FAC2	AS	τ (s)
1	1s ² 1S ₀	0.00000	0.00000	0.00000	0.00000	0.00000	0.00000
2	1s2s 3S ₁	797.34582	798.48352	796.97406	797.11176	797.11145	798.76208	4.281-10
3	1s2p 3P ₀ ^o	800.26160	801.12836	799.87250	800.04065	800.04053	801.28674	1.848-09
4	1s2s 1S ₀	800.43502	801.45300	800.13220	800.27991	800.27954	801.83307	1.345-03
5	1s2p 3P ₁ ^o	800.46973	801.62323	800.07312	800.25043	800.25031	801.79297	4.269-15
6	1s2p 3P ₂ ^o	803.56011	804.86084	803.28619	803.45416	803.45398	805.02167	1.941-11
7	1s2p 1P ₁ ^o	805.17105	806.45795	804.90912	805.09967	805.09955	806.68280	8.956-16
8	1s3s 3S ₁	945.39582	946.65387	945.08112	945.23901	945.23883	946.94891	1.239-13
9	1s3p 3P ₀ ^o	946.19956	947.38519	945.87970	946.03967	946.03955	947.63403	4.122-14
10	1s3s 1S ₀	946.21232	947.43805	945.92023	946.07190	946.07166	947.70905	1.236-13
11	1s3p 3P ₁ ^o	946.25059	947.52148	945.93640	946.09845	946.09827	947.76471	1.100-14
12	1s3p 3P ₂ ^o	947.19649	948.48816	946.89569	947.05701	947.05695	948.69220	4.343-14
13	1s3d 3D ₁		948.88940	947.31073	947.46228	947.46228	949.08521	1.434-14
14	1s3d 3D ₂		948.89960	947.29333	947.44543	947.44543	949.09668	1.430-14
15	1s3p 1P ₁ ^o	947.62570	948.92029	947.33972	947.50256	947.50244	949.12433	3.026-15
16	1s3d 3D ₃	948.02483	949.23773	947.63397	947.78534	947.78534	949.44379	1.463-14
17	1s3d 1D ₂	948.05855	949.25452	947.66754	947.81982	947.81982	949.46222	1.460-14
18	1s4s 3S ₁	996.69743	997.99231	996.40552	996.55450	996.55432	998.25989	1.830-13
19	1s4p 3P ₀ ^o	997.93277	998.29315	996.73328	996.87506	996.87506	998.53888	7.088-14
20	1s4s 1S ₀	997.02822	998.31085	996.74725	996.89166	996.89142	998.55237	1.722-13
21	1s4p 3P ₁ ^o	997.05373	998.34918	996.75690	996.89948	996.89941	998.58966	2.400-14
22	1s4p 3P ₂ ^o	997.44649	998.75720	997.16187	997.30493	997.30481	998.96649	7.407-14
23	1s4d 3D ₁		998.92188	997.33270	997.48724	997.48724	999.12457	3.333-14
24	1s4d 3D ₂		998.92731	997.32654	997.48126	997.48138	999.13049	3.322-14
25	1s4p 1P ₁ ^o	997.62874	998.93420	997.34442	997.48712	997.48694	999.13831	7.137-15
26	1s4d 3D ₃		999.06903	997.46918	997.62323	997.62323	999.27405	3.408-14
27	1s4d 1D ₂		999.07819	997.48535	997.63983	997.63983	999.28149	3.391-14
28	1s4f 3F ₂ ^o		999.07898	997.48499	997.63007	997.63007	999.28387	6.838-14
29	1s4f 3F ₃ ^o		999.07904	997.47980	997.62482	997.62482	999.28143	6.836-14
30	1s4f 3F ₄ ^o		999.15198	997.55322	997.69824	997.69824	999.35663	6.881-14
31	1s4f 1F ₃ ^o		999.15210	997.55725	997.70227	997.70227	999.35681	6.885-14
32	1s5s 3S ₁	1020.30744	1021.61121	1020.01941	1020.16406	1020.16388	1021.86420	2.962-13
33	1s5p 3P ₀ ^o	1020.47694	1021.76324	1020.18488	1020.32477	1020.32471	1022.00391	1.225-13
34	1s5s 1S ₀	1020.47147	1021.77209	1020.19226	1020.33350	1020.33301	1022.00189	2.458-13
35	1s5p 3P ₁ ^o	1020.48696	1021.79169	1020.19696	1020.33722	1020.33716	1022.02777	4.702-14
36	1s5p 3P ₂ ^o	1020.68835	1022.00037	1020.40417	1020.54462	1020.54449	1022.21088	1.277-13
37	1s5d 3D ₁		1022.08356	1020.49054	1020.64294	1020.64294	1022.28912	6.421-14
38	1s5d 3D ₂		1022.08655	1020.48761	1020.64026	1020.64026	1022.29230	6.345-14
39	1s5p 1P ₁ ^o	1020.78039	1022.09009	1020.49677	1020.63660	1020.63641	1022.29474	1.463-14
40	1s5d 3D ₃		1022.15894	1020.56042	1020.71252	1020.71252	1022.36395	6.586-14
41	1s5d 1D ₂		1022.16406	1020.56915	1020.72150	1020.72150	1022.36816	6.421-14
42	1s5f 3F ₂ ^o		1022.16449	1020.56897	1020.71362	1020.71362	1022.36932	1.319-13
43	1s5f 3F ₃ ^o		1022.16455	1020.56635	1020.71100	1020.71100	1022.36810	1.320-13
44	1s5f 3F ₄ ^o		1022.20190	1020.60394	1020.74854	1020.74854	1022.40625	1.329-13
45	1s5f 1F ₃ ^o		1022.20197	1020.60602	1020.75061	1020.75061	1022.40637	1.329-13
46	1s5g 3G ₃		1022.20203	1020.60577	1020.75012	1020.75012	1022.40533	2.228-13
47	1s5g 3G ₄		1022.20203	1020.60425	1020.74854	1020.74860	1022.40533	2.228-13
48	1s5g 3G ₅		1022.22437	1020.62677	1020.77106	1020.77106	1022.42841	2.234-13

Table 1: d. Energy levels (in Ryd) of Se XXXIII and their lifetimes (τ , s). $a\pm b \equiv a \times 10^{\pm b}$.

Index	Configuration/Level	NIST	GRASP1	GRASP2	FAC1	FAC2	AS	τ (s)
1	1s ² 1S ₀	0.00000	0.00000	0.00000	0.00000	0.00000	0.00000
2	1s2s 3S ₁	847.96060	849.23895	847.58148	847.72168	847.72144	849.51550	3.150-10
3	1s2p 3P ₀ ^o	850.99949	851.97845	850.59851	850.76965	850.76959	852.12384	1.747-09
4	1s2s 1S ₀	851.16899	852.31256	850.86206	851.01196	851.01160	852.71826	1.064-03
5	1s2p 3P ₁ ^o	851.20918	852.50494	850.79877	850.97968	850.97961	852.66272	3.554-15
6	1s2p 3P ₂ ^o	854.73715	856.20563	854.47565	854.64679	854.64667	856.34576	1.527-11
7	1s2p 1P ₁ ^o	856.38873	857.83801	856.13965	856.33240	856.33221	858.04529	8.040-16
8	1s3s 3S ₁	1005.51485	1006.93396	1005.20636	1005.36725	1005.36713	1007.22571	1.091-13
9	1s3p 3P ₀ ^o	1006.35230	1007.69147	1006.03735	1006.20013	1006.20013	1007.93231	3.636-14
10	1s3s 1S ₀	1006.36232	1007.74530	1006.07794	1006.23242	1006.23224	1008.01617	1.089-13
11	1s3p 3P ₁ ^o	1006.40242	1007.83606	1006.09381	1006.25885	1006.25879	1008.07056	9.342-15
12	1s3p 3P ₂ ^o	1007.46131	1008.94080	1007.19128	1007.35559	1007.35553	1009.12634	3.843-14
13	1s3d 3D ₁	1007.99431	1009.35510	1007.62073	1007.77502	1007.77502	1009.53088	1.267-14
14	1s3d 3D ₂		1009.36566	1007.60101	1007.75592	1007.75592	1009.54279	1.262-14
15	1s3p 1P ₁ ^o	1007.92059	1009.38281	1007.64716	1007.81281	1007.81274	1009.56805	2.715-15
16	1s3d 3D ₃	1008.35800	1009.74933	1007.98737	1008.14160	1008.14160	1009.93610	1.294-14
17	1s3d 1D ₂	1008.39354	1009.76660	1008.02307	1008.17822	1008.17822	1009.95514	1.290-14
18	1s4s 3S ₁	1060.11159	1061.57275	1059.82959	1059.98145	1059.98120	1061.83191	1.611-13
19	1s4p 3P ₀ ^o	1060.46060	1061.88428	1060.17053	1060.31519	1060.31506	1062.11938	6.252-14
20	1s4s 1S ₀	1060.45422	1061.90222	1060.18445	1060.33167	1060.33142	1062.13513	1.519-13
21	1s4p 3P ₁ ^o	1060.48065	1061.94373	1060.19397	1060.33948	1060.33936	1062.17285	2.051-14
22	1s4p 3P ₂ ^o	1060.92808	1062.40991	1060.65723	1060.80322	1060.80310	1062.60095	6.552-14
23	1s4d 3D ₁		1062.57996	1060.83411	1060.99146	1060.99146	1062.76343	2.944-14
24	1s4d 3D ₂		1062.58557	1060.82690	1060.98462	1060.98462	1062.76965	2.932-14
25	1s4p 1P ₁ ^o		1062.59106	1060.84473	1060.99023	1060.99011	1062.77637	6.417-15
26	1s4d 3D ₃		1062.74658	1060.98889	1061.14575	1061.14575	1062.93225	3.014-14
27	1s4d 1D ₂		1062.75598	1061.00598	1061.16333	1061.16333	1062.93970	2.996-14
28	1s4f 3F ₂ ^o		1062.75684	1061.00562	1061.15344	1061.15344	1062.94238	6.042-14
29	1s4f 3F ₃ ^o		1062.75684	1060.99988	1061.14771	1061.14771	1062.93958	6.040-14
30	1s4f 3F ₄ ^o		1062.83948	1061.08289	1061.23083	1061.23083	1063.02466	6.082-14
31	1s4f 1F ₃ ^o		1062.83960	1061.08728	1061.23511	1061.23523	1063.02478	6.086-14
32	1s5s 3S ₁	1085.23431	1086.70789	1084.95898	1085.10657	1085.10632	1086.94958	2.603-13
33	1s5p 3P ₀ ^o	1085.41110	1086.86523	1085.13110	1085.27393	1085.27380	1087.09338	1.080-13
34	1s5s 1S ₀	1085.40563	1086.87415	1085.13855	1085.28247	1085.28210	1087.09192	2.177-13
35	1s5p 3P ₁ ^o	1085.42203	1086.89539	1085.14319	1085.28625	1085.28613	1087.11865	4.020-14
36	1s5p 3P ₂ ^o	1085.74553	1087.13391	1085.38013	1085.52356	1085.52332	1087.32605	1.129-13
37	1s5d 3D ₁		1087.21973	1085.46960	1085.62488	1085.62488	1087.40637	5.670-14
38	1s5d 3D ₂		1087.22290	1085.46619	1085.62158	1085.62158	1087.40967	5.597-14
39	1s5p 1P ₁ ^o		1087.22559	1085.47522	1085.61792	1085.61780	1087.41150	1.311-14
40	1s5d 3D ₃		1087.30505	1085.54883	1085.70386	1085.70386	1087.49072	5.824-14
41	1s5d 1D ₂		1087.31030	1085.55811	1085.71326	1085.71326	1087.49512	5.671-14
42	1s5f 3F ₂ ^o		1087.31079	1085.55786	1085.70544	1085.70544	1087.49634	1.165-13
43	1s5f 3F ₃ ^o		1087.31091	1085.55505	1085.70239	1085.70239	1087.49487	1.166-13
44	1s5f 3F ₄ ^o		1087.35315	1085.59753	1085.74487	1085.74487	1087.53796	1.174-13
45	1s5f 1F ₃ ^o		1087.35315	1085.59985	1085.74719	1085.74719	1087.53809	1.175-13
46	1s5g 3G ₃		1087.35327	1085.59961	1085.74670	1085.74670	1087.53711	1.969-13
47	1s5g 3G ₄		1087.35327	1085.59790	1085.74500	1085.74500	1087.53711	1.969-13
48	1s5g 3G ₅		1087.37854	1085.62329	1085.77051	1085.77051	1087.56311	1.975-13

Table 1: e. Energy levels (in Ryd) of Br XXXIV and their lifetimes (τ , s). $a\pm b \equiv a \times 10^{\pm b}$.

Index	Configuration/Level	NIST	GRASP1	GRASP2	FAC1	FAC2	AS	τ (s)
1	1s ² ¹ S ₀	0.00000	0.00000	0.00000	0.00000	0.00000	0.00000
2	1s2s ³ S ₁	900.19625	901.62781	899.81268	899.95477	899.95453	901.89984	2.338-10
3	1s2p ³ P ₀ ^o	903.35862	904.46326	902.95123	903.12457	903.12451	904.59241	1.652-09
4	1s2s ¹ S ₀	903.52584	904.80664	903.21796	903.36945	903.36914	905.24097	8.463-04
5	1s2p ³ P ₁ ^o	903.57058	905.02130	903.14862	903.33252	903.33234	905.16406	2.988-15
6	1s2p ³ P ₂ ^o	907.58070	909.23376	907.33832	907.51196	907.51178	909.34802	1.209-11
7	1s2p ¹ P ₁ ^o	909.27329	910.90149	909.04401	909.23810	909.23798	911.08606	7.240-16
8	1s3s ³ S ₁	1067.56849	1069.16479	1067.27222	1067.43542	1067.43518	1069.45044	9.630-14
9	1s3p ³ P ₀ ^o	1068.44057	1069.94873	1068.13647	1068.30127	1068.30127	1070.17847	3.218-14
10	1s3s ¹ S ₀	1068.44786	1070.00366	1068.17688	1068.33350	1068.33325	1070.27258	9.623-14
11	1s3p ³ P ₁ ^o	1068.48978	1070.10168	1068.19202	1068.35925	1068.35913	1070.32410	7.994-15
12	1s3p ³ P ₂ ^o	1069.69265	1071.35901	1069.44214	1069.60864	1069.60864	1071.52100	3.414-14
13	1s3d ³ D ₁		1071.78638	1069.88599	1070.04248	1070.04248	1071.93677	1.123-14
14	1s3d ³ D ₂		1071.79724	1069.86377	1070.02075	1070.02075	1071.94910	1.118-14
15	1s3p ¹ P ₁ ^o	1070.16469	1071.81091	1069.91003	1070.07776	1070.07764	1071.97241	2.444-15
16	1s3d ³ D ₃		1072.23083	1070.30029	1070.45667	1070.45667	1072.39319	1.149-14
17	1s3d ¹ D ₂		1072.24866	1070.33826	1070.49548	1070.49548	1072.41284	1.144-14
18	1s4s ³ S ₁	1125.56790	1127.21277	1125.30298	1125.45703	1125.45691	1127.45984	1.422-13
19	1s4p ³ P ₀ ^o	1125.93150	1127.53516	1125.65747	1125.80408	1125.80408	1127.75574	5.534-14
20	1s4s ¹ S ₀	1125.92329	1127.55334	1125.67126	1125.82056	1125.82031	1127.77429	1.345-13
21	1s4p ³ P ₁ ^o	1125.95063	1127.59790	1125.68066	1125.82812	1125.82812	1127.81189	1.766-14
22	1s4p ³ P ₂ ^o	1126.45912	1128.12854	1126.20813	1126.35620	1126.35620	1128.29602	5.817-14
23	1s4d ³ D ₁		1128.30396	1126.39099	1126.55042	1126.55042	1128.46301	2.609-14
24	1s4d ³ D ₂		1128.30981	1126.38281	1126.54260	1126.54260	1128.46948	2.597-14
25	1s4p ¹ P ₁ ^o	1126.65231	1128.31372	1126.40063	1126.54822	1126.54810	1128.47510	5.785-15
26	1s4d ³ D ₃		1128.49182	1126.56604	1126.72498	1126.72498	1128.65295	2.676-14
27	1s4d ¹ D ₂		1128.50146	1126.58411	1126.74341	1126.74341	1128.66040	2.657-14
28	1s4f ³ F ₂ ^o		1128.50232	1126.58362	1126.73352	1126.73352	1128.66345	5.358-14
29	1s4f ³ F ₃ ^o		1128.50244	1126.57739	1126.72729	1126.72729	1128.66028	5.357-14
30	1s4f ³ F ₄ ^o		1128.59546	1126.67102	1126.82092	1126.82092	1128.75610	5.396-14
31	1s4f ¹ F ₃ ^o		1128.59558	1126.67578	1126.82568	1126.82568	1128.75623	5.399-14
32	1s5s ³ S ₁	1152.25436	1153.91357	1151.99756	1152.14722	1152.14697	1154.14014	2.296-13
33	1s5p ³ P ₀ ^o	1152.43752	1154.07654	1152.17651	1152.32117	1152.32117	1154.28821	9.553-14
34	1s5s ¹ S ₀	1152.43205	1154.08545	1152.18384	1152.32983	1152.32947	1154.28723	1.935-13
35	1s5p ³ P ₁ ^o	1152.44846	1154.10828	1152.18835	1152.33350	1152.33337	1154.31445	3.460-14
36	1s5p ³ P ₂ ^o	1152.70908	1154.37964	1152.45825	1152.60364	1152.60352	1154.54846	1.002-13
37	1s5d ³ D ₁		1154.46826	1152.55066	1152.70801	1152.70801	1154.63086	5.024-14
38	1s5d ³ D ₂		1154.47156	1152.54675	1152.70435	1152.70435	1154.63428	4.956-14
39	1s5p ¹ P ₁ ^o	1152.80658	1154.47351	1152.55591	1152.70056	1152.70032	1154.63550	1.178-14
40	1s5d ³ D ₃		1154.56445	1152.64026	1152.79724	1152.79724	1154.72571	5.169-14
41	1s5d ¹ D ₂		1154.56995	1152.65002	1152.80725	1152.80725	1154.72998	5.028-14
42	1s5f ³ F ₂ ^o		1154.57043	1152.64978	1152.79932	1152.79932	1154.73145	1.033-13
43	1s5f ³ F ₃ ^o		1154.57043	1152.64661	1152.79614	1152.79614	1154.72986	1.034-13
44	1s5f ³ F ₄ ^o		1154.61804	1152.69458	1152.84399	1152.84412	1154.77832	1.042-13
45	1s5f ¹ F ₃ ^o		1154.61816	1152.69702	1152.84656	1152.84656	1154.77844	1.042-13
46	1s5g ³ G ₃		1154.61816	1152.69678	1152.84595	1152.84595	1154.77722	1.747-13
47	1s5g ³ G ₄		1154.61816	1152.69495	1152.84412	1152.84412	1154.77722	1.747-13
48	1s5g ³ G ₅		1154.64673	1152.72363	1152.87280	1152.87280	1154.80652	1.753-13

Table 3: a. Collision strengths for transitions in Ga XXX. ($a \pm b \equiv a \times 10^{\pm b}$).

Transition		Energy (Ryd)					
i	j	900	1200	1500	1800	2100	FAC ^a
1	2	2.038-04	1.462-04	1.094-04	8.475-05	6.927-05	7.760-05
1	3	1.182-04	7.456-05	5.071-05	3.585-05	2.683-05	3.192-05
1	4	6.395-04	7.418-04	8.145-04	8.656-04	9.152-04	7.652-04
1	5	6.197-04	6.550-04	7.202-04	7.941-04	8.706-04	9.110-04
1	6	5.386-04	3.352-04	2.256-04	1.580-04	1.173-04	1.506-04
1	7	2.084-03	3.016-03	3.821-03	4.535-03	5.174-03	4.637-03
1	8	6.533-05	4.557-05	3.321-05	2.534-05	2.039-05	2.073-05
1	9	3.945-05	2.432-05	1.621-05	1.130-05	8.370-06	8.770-06
1	10	1.091-04	1.353-04	1.526-04	1.650-04	1.766-04	1.489-04
1	11	1.474-04	1.387-04	1.433-04	1.528-04	1.648-04	1.779-04
1	12	1.828-04	1.111-04	7.319-05	5.052-05	3.712-05	4.176-05
1	13	1.558-05	7.880-06	4.534-06	2.884-06	1.957-06	2.191-06
1	14	2.396-05	2.099-05	2.252-05	2.507-05	2.771-05	2.753-05
1	15	3.077-04	4.836-04	6.347-04	7.669-04	8.841-04	8.307-04
1	16	3.368-05	1.677-05	9.531-06	6.006-06	4.044-06	4.958-06
1	17	2.192-05	2.724-05	3.467-05	4.162-05	4.773-05	4.435-05
1	18	2.927-05	1.951-05	1.406-05	1.084-05	8.699-06	8.385-06
1	19	1.735-05	1.058-05	6.983-06	4.882-06	3.594-06	3.589-06
1	20	3.851-05	4.858-05	5.527-05	6.107-05	6.553-05	5.526-05
1	21	5.969-05	5.373-05	5.413-05	5.700-05	6.095-05	6.590-05
1	22	8.097-05	4.862-05	3.173-05	2.195-05	1.602-05	1.713-05
1	23	9.235-06	4.567-06	2.603-06	1.654-06	1.115-06	1.186-06
1	24	1.337-05	1.032-05	1.047-05	1.144-05	1.258-05	1.276-05
1	25	1.032-04	1.682-04	2.239-04	2.724-04	3.152-04	2.989-04
1	26	2.005-05	9.758-06	5.490-06	3.453-06	2.310-06	2.688-06
1	27	1.134-05	1.274-05	1.608-05	1.943-05	2.246-05	2.135-05
1	28	6.393-07	2.494-07	1.227-07	6.916-08	4.287-08	4.771-08
1	29	7.822-07	4.054-07	3.355-07	3.273-07	3.337-07	3.244-07
1	30	1.073-06	4.116-07	2.004-07	1.121-07	6.910-08	8.406-08
1	31	7.281-07	4.202-07	3.926-07	4.100-07	4.331-07	3.999-07
1	32	1.651-05	1.005-05	7.175-06	5.503-06	4.410-06	4.171-06
1	33	9.155-06	5.482-06	3.603-06	2.501-06	1.847-06	1.802-06
1	34	1.911-05	2.358-05	2.688-05	2.969-05	3.208-05	2.697-05
1	35	3.060-05	2.670-05	2.659-05	2.779-05	2.965-05	3.193-05
1	36	4.291-05	2.528-05	1.643-05	1.128-05	8.260-06	8.596-06
1	37	5.541-06	2.637-06	1.498-06	9.478-07	6.393-07	6.644-07
1	38	8.011-06	5.600-06	5.518-06	5.959-06	6.526-06	6.675-06
1	39	4.896-05	8.006-05	1.072-04	1.306-04	1.514-04	1.434-04
1	40	1.208-05	5.643-06	3.165-06	1.982-06	1.326-06	1.506-06
1	41	6.743-06	6.724-06	8.415-06	1.018-05	1.180-05	1.135-05
1	42	5.849-07	2.078-07	1.019-07	5.733-08	3.552-08	3.871-08
1	43	7.338-07	3.271-07	2.602-07	2.501-07	2.556-07	2.496-07
1	44	9.845-07	3.434-07	1.667-07	9.302-08	5.729-08	6.823-08
1	45	6.939-07	3.359-07	3.016-07	3.121-07	3.317-07	3.081-07
1	46	1.956-08	4.033-09	1.614-09	7.745-10	4.241-10	4.864-10
1	47	2.461-08	5.978-09	3.393-09	2.663-09	2.598-09	2.091-09
1	48	2.893-08	5.825-09	2.307-09	1.098-09	5.984-10	7.523-10

Table 3: b. Collision strengths for transitions in Ge XXXI. ($a \pm b \equiv a \times 10^{\pm b}$).

Transition		Energy (Ryd)						
i	j	1000	1250	1500	1750	2000	2250	FAC ^a
1	2	1.831-04	1.414-04	1.124-04	9.138-05	7.501-05	6.333-05	7.219-05
1	3	1.047-04	7.323-05	5.374-05	4.027-05	3.147-05	2.527-05	2.965-05
1	4	6.151-04	6.927-04	7.514-04	7.937-04	8.305-04	8.672-04	7.202-04
1	5	6.075-04	6.444-04	6.990-04	7.585-04	8.224-04	8.855-04	9.258-04
1	6	4.735-04	3.272-04	2.380-04	1.770-04	1.371-04	1.094-04	1.393-04
1	7	2.049-03	2.719-03	3.320-03	3.862-03	4.363-03	4.822-03	4.331-03
1	8	5.860-05	4.390-05	3.418-05	2.766-05	2.256-05	1.905-05	1.930-05
1	9	3.499-05	2.390-05	1.723-05	1.278-05	9.928-06	7.927-06	8.151-06
1	10	1.063-04	1.247-04	1.392-04	1.501-04	1.591-04	1.680-04	1.400-04
1	11	1.396-04	1.351-04	1.390-04	1.462-04	1.557-04	1.658-04	1.789-04
1	12	1.611-04	1.087-04	7.755-05	5.706-05	4.395-05	3.485-05	3.868-05
1	13	1.347-05	7.866-06	5.021-06	3.424-06	2.461-06	1.833-06	2.023-06
1	14	2.175-05	1.977-05	2.062-05	2.240-05	2.439-05	2.637-05	2.629-05
1	15	3.088-04	4.345-04	5.470-04	6.474-04	7.396-04	8.235-04	7.757-04
1	16	2.889-05	1.667-05	1.052-05	7.110-06	5.075-06	3.755-06	4.569-06
1	17	2.082-05	2.481-05	3.016-05	3.549-05	4.037-05	4.475-05	4.174-05
1	18	2.584-05	1.901-05	1.459-05	1.178-05	9.532-06	7.895-06	7.806-06
1	19	1.538-05	1.045-05	7.468-06	5.527-06	4.241-06	3.369-06	3.336-06
1	20	3.757-05	4.509-05	5.034-05	5.473-05	5.836-05	6.156-05	5.194-05
1	21	5.589-05	5.229-05	5.262-05	5.467-05	5.760-05	6.109-05	6.604-05
1	22	7.133-05	4.784-05	3.385-05	2.484-05	1.889-05	1.491-05	1.587-05
1	23	7.928-06	4.581-06	2.897-06	1.969-06	1.404-06	1.044-06	1.096-06
1	24	1.183-05	9.820-06	9.727-06	1.032-05	1.113-05	1.199-05	1.221-05
1	25	1.045-04	1.507-04	1.924-04	2.296-04	2.629-04	2.939-04	2.790-04
1	26	1.709-05	9.743-06	6.092-06	4.100-06	2.904-06	2.144-06	2.479-06
1	27	1.044-05	1.166-05	1.399-05	1.648-05	1.886-05	2.102-05	2.008-05
1	28	5.201-07	2.547-07	1.423-07	8.748-08	5.750-08	3.988-08	4.383-08
1	29	6.404-07	3.943-07	3.244-07	3.072-07	3.074-07	3.131-07	3.063-07
1	30	8.663-07	4.186-07	2.318-07	1.414-07	9.238-08	6.380-08	7.712-08
1	31	5.965-07	4.021-07	3.668-07	3.727-07	3.893-07	4.067-07	3.776-07
1	32	1.387-05	9.845-06	7.449-06	6.018-06	4.923-06	4.044-06	3.884-06
1	33	8.123-06	5.404-06	3.844-06	2.834-06	2.193-06	1.734-06	1.676-06
1	34	1.844-05	2.175-05	2.443-05	2.657-05	2.858-05	2.998-05	2.534-05
1	35	2.852-05	2.591-05	2.580-05	2.665-05	2.805-05	2.968-05	3.194-05
1	36	3.780-05	2.483-05	1.748-05	1.278-05	9.797-06	7.695-06	7.971-06
1	37	4.664-06	2.640-06	1.664-06	1.128-06	8.066-07	5.974-07	6.140-07
1	38	6.825-06	5.342-06	5.157-06	5.400-06	5.796-06	6.226-06	6.393-06
1	39	4.961-05	7.157-05	9.171-05	1.098-04	1.260-04	1.412-04	1.339-04
1	40	1.007-05	5.625-06	3.504-06	2.354-06	1.670-06	1.229-06	1.389-06
1	41	5.856-06	6.161-06	7.328-06	8.630-06	9.893-06	1.105-05	1.066-05
1	42	4.407-07	2.119-07	1.182-07	7.255-08	4.768-08	3.301-08	3.558-08
1	43	5.537-07	3.193-07	2.537-07	2.358-07	2.352-07	2.400-07	2.356-07
1	44	7.352-07	3.489-07	1.927-07	1.174-07	7.666-08	5.285-08	6.261-08
1	45	5.198-07	3.228-07	2.837-07	2.842-07	2.970-07	3.117-07	2.909-07
1	46	1.154-08	4.197-09	1.985-09	1.060-09	6.229-10	3.943-10	4.442-10
1	47	1.515-08	6.024-09	3.629-09	2.724-09	2.414-09	2.385-09	1.970-09
1	48	1.683-08	6.037-09	2.828-09	1.499-09	8.759-10	5.524-10	6.862-10

Table 3: c. Collision strengths for transitions in As XXXII. ($a\pm b \equiv a\times 10^{\pm b}$).

Transition		Energy (Ryd)						
i	j	1100	1400	1700	2000	2300	2600	FAC ^a
1	2	1.681-04	1.254-04	9.695-05	7.778-05	6.367-05	5.333-05	6.734-05
1	3	9.376-05	6.353-05	4.526-05	3.359-05	2.589-05	2.048-05	2.763-05
1	4	5.950-04	6.689-04	7.265-04	7.704-04	8.122-04	8.460-04	6.795-04
1	5	5.975-04	6.516-04	7.211-04	7.947-04	8.697-04	9.419-04	9.364-04
1	6	4.205-04	2.816-04	1.981-04	1.458-04	1.113-04	8.736-05	1.293-04
1	7	1.992-03	2.675-03	3.286-03	3.833-03	4.335-03	4.794-03	4.052-03
1	8	5.347-05	3.897-05	2.955-05	2.325-05	1.921-05	1.582-05	1.801-05
1	9	3.115-05	2.072-05	1.448-05	1.060-05	8.135-06	6.376-06	7.599-06
1	10	1.035-04	1.222-04	1.356-04	1.459-04	1.566-04	1.647-04	1.320-04
1	11	1.325-04	1.325-04	1.396-04	1.499-04	1.618-04	1.735-04	1.792-04
1	12	1.423-04	9.339-05	6.449-05	4.675-05	3.557-05	2.764-05	3.594-05
1	13	1.182-05	6.580-06	4.057-06	2.710-06	1.921-06	1.408-06	1.874-06
1	14	1.995-05	1.874-05	2.009-05	2.218-05	2.435-05	2.642-05	2.512-05
1	15	3.034-04	4.325-04	5.459-04	6.471-04	7.389-04	8.214-04	7.259-04
1	16	2.520-05	1.381-05	8.411-06	5.565-06	3.909-06	2.848-06	4.224-06
1	17	1.979-05	2.447-05	3.015-05	3.561-05	4.046-05	4.480-05	3.937-05
1	18	2.360-05	1.668-05	1.268-05	9.956-06	7.970-06	6.608-06	7.287-06
1	19	1.378-05	9.002-06	6.294-06	4.591-06	3.461-06	2.722-06	3.111-06
1	20	3.696-05	4.382-05	4.974-05	5.388-05	5.730-05	6.055-05	4.893-05
1	21	5.272-05	5.058-05	5.231-05	5.557-05	5.949-05	6.373-05	6.594-05
1	22	6.341-05	4.086-05	2.822-05	2.038-05	1.524-05	1.188-05	1.476-05
1	23	6.987-06	3.809-06	2.344-06	1.557-06	1.095-06	8.022-07	1.016-06
1	24	1.074-05	9.140-06	9.388-06	1.018-05	1.110-05	1.204-05	1.169-05
1	25	1.035-04	1.507-04	1.923-04	2.296-04	2.634-04	2.940-04	2.611-04
1	26	1.495-05	8.026-06	4.879-06	3.208-06	2.237-06	1.628-06	2.292-06
1	27	9.809-06	1.142-05	1.398-05	1.658-05	1.895-05	2.111-05	1.892-05
1	28	4.418-07	2.046-07	1.105-07	6.629-08	4.277-08	2.937-08	4.040-08
1	29	5.510-07	3.440-07	2.951-07	2.876-07	2.917-07	3.004-07	2.897-07
1	30	7.303-07	3.334-07	1.781-07	1.060-07	6.802-08	4.649-08	7.097-08
1	31	5.148-07	3.601-07	3.438-07	3.575-07	3.761-07	3.953-07	3.571-07
1	32	1.241-05	8.669-06	6.412-06	5.071-06	4.084-06	3.346-06	3.627-06
1	33	7.165-06	4.656-06	3.229-06	2.350-06	1.782-06	1.392-06	1.563-06
1	34	1.775-05	2.118-05	2.406-05	2.610-05	2.788-05	2.955-05	2.386-05
1	35	2.643-05	2.493-05	2.552-05	2.699-05	2.887-05	3.083-05	3.185-05
1	36	3.312-05	2.121-05	1.453-05	1.047-05	7.868-06	6.091-06	7.412-06
1	37	4.045-06	2.196-06	1.343-06	8.921-07	6.269-07	4.580-07	5.690-07
1	38	6.060-06	4.933-06	4.947-06	5.315-06	5.775-06	6.252-06	6.125-06
1	39	4.879-05	7.153-05	9.179-05	1.099-04	1.264-04	1.411-04	1.252-04
1	40	8.676-06	4.634-06	2.802-06	1.841-06	1.282-06	9.309-07	1.285-06
1	41	5.366-06	6.015-06	7.316-06	8.686-06	9.950-06	1.111-05	1.005-05
1	42	3.673-07	1.702-07	9.168-08	5.498-08	3.543-08	2.432-08	3.280-08
1	43	4.638-07	2.758-07	2.287-07	2.199-07	2.234-07	2.309-07	2.229-07
1	44	6.081-07	2.778-07	1.480-07	8.803-08	5.639-08	3.854-08	5.764-08
1	45	4.351-07	2.856-07	2.639-07	2.720-07	2.876-07	3.041-07	2.752-07
1	46	8.920-09	3.219-09	1.456-09	7.558-10	4.362-10	2.742-10	4.070-10
1	47	1.173-08	4.819-09	2.966-09	2.342-09	2.195-09	2.240-09	1.853-09
1	48	1.291-08	4.591-09	2.054-09	1.058-09	6.073-10	3.803-10	6.281-10

Table 3: d. Collision strengths for transitions in Se XXXIII. ($a \pm b \equiv a \times 10^{\pm b}$).

Transition		Energy (Ryd)					
i	j	1100	1500	2000	2500	3000	FAC ^a
1	2	1.688-04	1.178-04	8.198-05	5.882-05	4.510-05	6.298-05
1	3	9.769-05	5.972-05	3.578-05	2.360-05	1.654-05	2.582-05
1	4	5.430-04	6.415-04	7.215-04	7.767-04	8.292-04	6.421-04
1	5	5.752-04	6.483-04	7.653-04	8.856-04	1.001-03	9.430-04
1	6	4.367-04	2.620-04	1.545-04	1.005-04	6.952-05	1.203-04
1	7	1.705-03	2.516-03	3.378-03	4.119-03	4.775-03	3.799-03
1	8	5.414-05	3.627-05	2.472-05	1.736-05	1.347-05	1.685-05
1	9	3.260-05	1.932-05	1.131-05	7.350-06	5.127-06	7.104-06
1	10	9.269-05	1.162-04	1.357-04	1.496-04	1.619-04	1.246-04
1	11	1.287-04	1.292-04	1.439-04	1.628-04	1.824-04	1.789-04
1	12	1.487-04	8.641-05	4.973-05	3.183-05	2.191-05	3.348-05
1	13	1.276-05	6.077-06	2.994-06	1.718-06	1.094-06	1.741-06
1	14	1.964-05	1.769-05	2.023-05	2.348-05	2.655-05	2.403-05
1	15	2.544-04	4.068-04	5.670-04	7.028-04	8.221-04	6.807-04
1	16	2.713-05	1.266-05	6.120-06	3.465-06	2.183-06	3.915-06
1	17	1.806-05	2.311-05	3.142-05	3.874-05	4.490-05	3.722-05
1	18	2.407-05	1.561-05	1.039-05	7.375-06	5.598-06	6.820-06
1	19	1.434-05	8.413-06	4.860-06	3.161-06	2.189-06	2.909-06
1	20	3.266-05	4.186-05	4.954-05	5.489-05	5.991-05	4.616-05
1	21	5.122-05	4.912-05	5.323-05	5.976-05	6.661-05	6.563-05
1	22	6.594-05	3.792-05	2.152-05	1.378-05	9.420-06	1.375-05
1	23	7.552-06	3.529-06	1.721-06	9.803-07	6.227-07	9.439-07
1	24	1.084-05	8.624-06	9.335-06	1.073-05	1.214-05	1.120-05
1	25	8.576-05	1.418-04	2.008-04	2.508-04	2.943-04	2.449-04
1	26	1.615-05	7.384-06	3.531-06	1.983-06	1.246-06	2.126-06
1	27	9.241-06	1.078-05	1.459-05	1.816-05	2.123-05	1.787-05
1	28	5.086-07	1.882-07	7.589-08	3.788-08	2.180-08	3.734-08
1	29	6.117-07	3.194-07	2.700-07	2.762-07	2.896-07	2.744-07
1	30	8.312-07	3.047-07	1.209-07	5.971-08	3.415-08	6.550-08
1	31	5.676-07	3.352-07	3.284-07	3.577-07	3.851-07	3.383-07
1	32	1.323-05	8.043-06	5.343-06	3.761-06	2.820-06	3.395-06
1	33	7.637-06	4.383-06	2.504-06	1.622-06	1.116-06	1.462-06
1	34	1.613-05	2.040-05	2.400-05	2.667-05	2.912-05	2.249-05
1	35	2.628-05	2.423-05	2.587-05	2.895-05	3.216-05	3.166-05
1	36	3.528-05	1.983-05	1.113-05	7.098-06	4.822-06	6.911-06
1	37	4.516-06	2.043-06	9.869-07	5.620-07	3.553-07	5.289-07
1	38	6.378-06	4.659-06	4.893-06	5.582-06	6.310-06	5.871-06
1	39	4.088-05	6.737-05	9.596-05	1.204-04	1.413-04	1.174-04
1	40	9.691-06	4.283-06	2.028-06	1.139-06	7.126-07	1.192-06
1	41	5.344-06	5.680-06	7.638-06	9.531-06	1.118-05	9.488-06
1	42	4.472-07	1.572-07	6.291-08	3.141-08	1.806-08	3.033-08
1	43	5.451-07	2.570-07	2.075-07	2.114-07	2.235-07	2.112-07
1	44	7.171-07	2.549-07	1.003-07	4.956-08	2.830-08	5.321-08
1	45	5.211-07	2.667-07	2.506-07	2.736-07	2.977-07	2.607-07
1	46	1.292-08	2.950-09	9.123-10	3.792-10	1.922-10	3.741-10
1	47	1.662-08	4.415-09	2.344-09	2.031-09	2.138-09	1.746-09
1	48	1.848-08	4.179-09	1.272-09	5.236-10	2.640-10	5.766-10

Table 3: e. Collision strengths for transitions in Br XXXIV. ($a \pm b \equiv a \times 10^{\pm b}$).

Transition		Energy (Ryd)						
i	j	1200	1600	2000	2400	2800	3200	FAC ^a
1	2	1.557-04	1.105-04	8.404-05	6.450-05	5.230-05	4.178-05	5.905-05
1	3	8.866-05	5.595-05	3.776-05	2.697-05	2.022-05	1.563-05	2.419-05
1	4	5.262-04	6.075-04	6.740-04	7.179-04	7.597-04	7.883-04	6.077-04
1	5	5.638-04	6.411-04	7.325-04	8.267-04	9.178-04	1.007-03	9.459-04
1	6	3.930-04	2.438-04	1.620-04	1.144-04	8.491-05	6.501-05	1.122-04
1	7	1.651-03	2.360-03	2.978-03	3.529-03	4.024-03	4.487-03	3.569-03
1	8	5.012-05	3.424-05	2.571-05	1.959-05	1.547-05	1.228-05	1.580-05
1	9	2.977-05	1.820-05	1.208-05	8.517-06	6.305-06	4.861-06	6.659-06
1	10	9.115-05	1.105-04	1.266-04	1.371-04	1.472-04	1.536-04	1.178-04
1	11	1.235-04	1.263-04	1.377-04	1.520-04	1.670-04	1.823-04	1.780-04
1	12	1.346-04	8.084-05	5.287-05	3.681-05	2.694-05	2.057-05	3.127-05
1	13	1.138-05	5.695-06	3.304-06	2.102-06	1.428-06	1.028-06	1.622-06
1	14	1.819-05	1.677-05	1.849-05	2.083-05	2.315-05	2.538-05	2.300-05
1	15	2.505-04	3.830-04	4.977-04	5.990-04	6.894-04	7.736-04	6.398-04
1	16	2.403-05	1.178-05	6.729-06	4.226-06	2.846-06	2.032-06	3.638-06
1	17	1.722-05	2.182-05	2.774-05	3.327-05	3.812-05	4.247-05	3.525-05
1	18	2.226-05	1.483-05	1.082-05	8.152-06	6.502-06	5.091-06	6.398-06
1	19	1.322-05	7.955-06	5.176-06	3.631-06	2.688-06	2.058-06	2.727-06
1	20	3.237-05	4.003-05	4.581-05	5.006-05	5.393-05	5.643-05	4.363-05
1	21	4.906-05	4.780-05	5.084-05	5.571-05	6.090-05	6.635-05	6.513-05
1	22	6.031-05	3.562-05	2.283-05	1.582-05	1.157-05	8.773-06	1.285-05
1	23	6.766-06	3.317-06	1.893-06	1.202-06	8.122-07	5.840-07	8.796-07
1	24	9.954-06	8.182-06	8.598-06	9.551-06	1.060-05	1.163-05	1.073-05
1	25	8.523-05	1.335-04	1.755-04	2.130-04	2.460-04	2.768-04	2.301-04
1	26	1.436-05	6.893-06	3.870-06	2.426-06	1.623-06	1.159-06	1.977-06
1	27	8.711-06	1.019-05	1.286-05	1.551-05	1.791-05	2.008-05	1.692-05
1	28	4.461-07	1.763-07	8.636-08	4.892-08	3.038-08	2.035-08	3.462-08
1	29	5.424-07	3.001-07	2.565-07	2.553-07	2.637-07	2.741-07	2.604-07
1	30	7.311-07	2.835-07	1.370-07	7.686-08	4.742-08	3.159-08	6.062-08
1	31	4.996-07	3.150-07	3.042-07	3.231-07	3.450-07	3.650-07	3.210-07
1	32	1.181-05	7.695-06	5.519-06	4.201-06	3.295-06	2.644-06	3.185-06
1	33	6.818-06	4.103-06	2.680-06	1.868-06	1.385-06	1.056-06	1.371-06
1	34	1.538-05	1.924-05	2.230-05	2.429-05	2.633-05	2.750-05	2.125-05
1	35	2.438-05	2.344-05	2.477-05	2.696-05	2.947-05	3.200-05	3.137-05
1	36	3.125-05	1.845-05	1.187-05	8.168-06	5.986-06	4.513-06	6.460-06
1	37	3.891-06	1.911-06	1.091-06	6.881-07	4.658-07	3.333-07	4.929-07
1	38	5.620-06	4.406-06	4.526-06	4.986-06	5.515-06	6.052-06	5.631-06
1	39	3.987-05	6.344-05	8.390-05	1.020-04	1.181-04	1.329-04	1.103-04
1	40	8.284-06	3.979-06	2.236-06	1.391-06	9.325-07	6.624-07	1.108-06
1	41	4.800-06	5.361-06	6.727-06	8.131-06	9.410-06	1.058-05	8.976-06
1	42	3.697-07	1.467-07	7.187-08	4.053-08	2.519-08	1.686-08	2.812-08
1	43	4.582-07	2.399-07	1.986-07	1.953-07	2.023-07	2.119-07	2.004-07
1	44	6.073-07	2.364-07	1.142-07	6.377-08	3.934-08	2.620-08	4.926-08
1	45	4.249-07	2.488-07	2.333-07	2.464-07	2.647-07	2.825-07	2.474-07
1	46	9.556-09	2.739-09	1.099-09	5.303-10	2.930-10	1.792-10	3.448-10
1	47	1.232-08	4.089-09	2.408-09	1.943-09	1.898-09	1.981-09	1.642-09
1	48	1.374-08	3.855-09	1.526-09	7.292-10	4.005-10	2.440-10	5.309-10